

**UNIVERSITY OF GAZIANTEP
GRADUATE SCHOOL OF
NATURAL AND APPLIED SCIENCES**

**NEURAL NETWORK MODELING OF
TORSIONAL STRENGTH OF RC BEAMS**

**M. Sc. THESIS
IN
CIVIL ENGINEERING**

**BY
Gökşen Melih DERELİ
January 2011**

**GAZİANTEP ÜNİVERSİTESİ
FEN BİLİMLERİ ENSTİTÜSÜ**

**BETONARME KİRİŞLERİN BURULMA
DAYANIMININ YAPAY SINIR AĞLARI İLE
MODELLENMESİ**

**İNŞAAT MÜHENDİSLİĞİ
YÜKSEK LİSANS**

**Gökşen Melih DERELİ
OCAK 2011**

**Neural Network Modeling of Torsional
Strength of RC Beams**

**M.Sc. Thesis
in
Civil Engineering
University of Gaziantep**

**Supervisor
Assoc. Prof. Dr. Abdulkadir EVİK**

**By
Gökşen Melih DERELİ
January 2011**

**Betonarme Kirişlerin Burulma Dayanımının
Yapay Sinir Ağları ile Modellenmesi**

**Gaziantep Üniversitesi
İnşaat Mühendisliği
Yüksek Lisans**

**Danışman
Doç. Dr. Abdulkadir ÇEVİK**

**Gökşen Melih DERELİ
Ocak 2011**

January 2011

M. Sc. In Civil Engineering

Gökşen Melih DERELİ

Ocak 2011

Yüksek Lisans - İnşaat Mühendisliği

Gökşen Melih DERELİ

T.C.
UNIVERSITY OF GAZİANTEP
GRADUATE SCHOOL OF
NATURAL & APPLIED SCIENCES
DEPARTMENT OF MECHANICS

Name of the thesis: Neural Network Modeling of Torsional Strength of Rc Beams
Name of the student: Gökşen Melih Dereli
Exam date: 21 January 2011

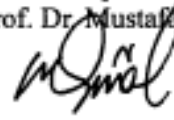
Approval of the Graduate School of Natural and Applied Sciences

Director
Prof. Dr. Ramazan KOÇ



I certify that this thesis satisfies all the requirements as a thesis for the degree of Master of Science of Philosophy.

Head of Department
Assoc. Prof. Dr. Mustafa GÜNAL



This is to certify that we have read this thesis and that in our consensus/majority opinion it is fully adequate, in scope and quality, as a thesis for the degree of Master of Science of Philosophy.

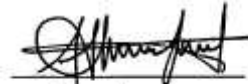
Supervisor
Assoc. Prof. Dr. Abdülkadir ÇEVİK



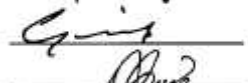
Examining Committee Members
Title and Name-surname

Signature

Prof. Dr. Mustafa ÖZAKÇA



Assoc. Prof. Dr. Abdülkadir ÇEVİK



Asist. Prof. Dr. Ahmet ERKLİĞ



ABSTRACT

NEURAL NETWORK MODELING OF TORSIONAL STRENGTH OF RC BEAMS

DERELİ, Gökşen Melih
M.Sc. in Civil Eng.

Supervisor: Assoc. Prof. Dr. Abdulkadir ÇEVİK
January 2011, 78 pages

This study presents the application of Neural Networks (NN) for modeling torsion of RC beams. The NN models are proposed for the computation of selected two different NN models. The proposed NN models are based on a wide range experimental database. The accuracy of the proposed NN models is quite satisfactory as compared to results of design codes. Moreover, the results of proposed NN formulations are compared with existing models and are found to be more accurate than the expression available in the literature. The generalization capability of proposed NN models is also verified by a set of parametric studies.

Keywords: Neural Networks, Torsional Strength, RC beams.

ÖZET

BETONARME KİRİŞLERİN BURULMA DAYANIMININ YAPAY SİNİR AĞLARI İLE MODELLENMESİ

DERELİ, Gökşen Melih
Yüksek Lisans Tezi, İnş Müh. Bölümü
Tez Yöneticisi: Doç. Dr. Abdulkadir ÇEVİK
Ocak 2011, 78 sayfa

Bu çalışmada betonarme kirişlerin yapay sinir ağları ile modellenmesi anlatılmıştır. Çalışmalar için iki farklı yapay sinir ağı modeli önerildi ve önerilen yapay sinir ağı modelleri geniş aralıklı deneysel veri tabanlarına dayandırıldı. Dizayn kodlarının sonuçları ile karşılaştırılan yapay sinir ağı modellerinin doğruluğunun oldukça memnuniyet verici olduğu görüldü. Ayrıca önerilen yapay sinir ağı modellerinin formüllerinin sonuçları var olan modellerle karşılaştırıldığında literatürdeki benzer çalışmalardan daha doğru olduğu bulundu. Önerilen yapay sinir ağı modellerinin genellenme kapasitesi parametrik çalışmalar tarafından doğrulandı.

Anahtar Kelimeler: Yapay Sinir Ağları, Burulma Dayanımı, Betonarme Kirişler.

ACKNOWLEDGMENTS

I express sincere appreciation to Assoc. Prof. Dr. Abdulkadir EVİK, my wife Meral DERELİ and my little child Alaz Toprak DERELİ.

CONTENTS	pages
ABSTRACT	i
ACKNOWLEDGMENTS	iii
CONTENTS	iv
LIST OF TABLES	vi
LIST OF FIGURES	vii
LIST OF SYMBOLS	viii
CHAPTER 1: INTRODUCTION	1
1.1 General Introduction	1
1.2 Layout of the Thesis	2
CHAPTER 2: LITERATURE REVIEW	4
2.1 Engineering Analysis	4
2.2 RC Beams	5
2.2.1 Advantages of Using High Strength Concrete	5
2.3 Neural Networks	6
2.3.1 Neural Networks in Structural Mechanics	7
CHAPTER 3 : THEORY OF TORSIONAL STRENGTH OF RC BEAMS	8
3.1 Torsional Strength	8
3.1.1 Torsional Strength and Torsion in the Building Standards	8
3.1.2 Pure Torsion in Concrete Elements	12
3.1.3 Torsion in Elastic Materials	14
3.1.4 Torsion in Plastic Materials	16
3.1.5 Sand-heap Analogy Applied to L Beams	17
3.1.6 Skew-Bending Theory	21
3.1.7 Torsion In Reinforced Concrete Elements	25
3.1.8 Space Truss Analogy Theory	26
3.1.9 Equilibrium in Element Shear	27
3.1.10 Equilibrium in Element Torsion	29
3.1.11 Shear-Torsion-Bending Interaction	30
3.2 Aci Design Of Reinforced Concrete Beams	32
3.2.1 Torsional Behavior of Structures	32
3.2.2 Torsional Moment Strength	33
CHAPTER 4 : NEURAL NETWORKS	34
4.1 Neural Networks Systems	34
4.1.1 Neural Networks	34
4.1.2 History of Neural Networks	36
4.1.3 Elements of Neural Networks	36
4.1.4 Classification of Neural Networks	39
4.1.5 Back propagation Algorithm	42

4.1.6 Matlab NN Toolbox	44
4.1.7 Optimal NN Model Selection	46
CHAPTER 5 : NUMERICAL APPLICATION	49
5.1 Selection of Database (Description of data)	49
5.2 Numerical Application of NN	49
5.3 Explicit Formulation of NN Model	53
5.4 Main Effects of Variables	55
CHAPTER 6 : CONCLUSION	65
6.1 Conclusion	65
6.2 Recommendations for Further Work	66
APPENDIX A - NN Model 1 Data	67
APPENDIX B - NN Model 2 Data	69
REFERENCES	71

LIST OF TABLES

	pages
Table 4.1. Back propagation training algorithms used in NN training	47
Table 5.1. Data Range	50
Table 5.2. Statistical parameters of testing and training sets and overall results of NN model 1	51
Table 5.3. Statistical parameters of testing and training sets and overall results of NN model 2	51
Table 5.4. Predicting capability of building code approaches	55

LIST OF FIGURES

	pages
Fig3.1 Thin-walled tube and space-truss analogy	9
Fig3.2 Skew-bending theory analogy	10
Fig3.3 The cross section of a rectangular reinforced concrete beam	12
Fig3.4 Torsional stress distribution through circular section	13
Fig3.5 Pure torsion stress distribution in a rectangular section	13
Fig3.6 Membrane analogy in elastic pure torsion	15
Fig3.7 Sand-heap analogy in plastic pure torsion	17
Fig3.8 Sand-heap analogy of flanged section	19
Fig3.9 Component rectangles for T_c calculation	22
Fig3.10 Skew bending due to torsion	23
Fig3.11 Forces on the skewly bent planes	24
Fig3.12 Forces on hollow box concrete surface by truss analogy	27
Fig3.13 Equilibrium forces in element shear	28
Fig3.14 Hollow tube equilibrium torsion forces	29
Fig3.15 Shear-torsion interaction diagram	31
Fig4.1 A biological neuron	37
Fig4.2 Artificial neuron model	37
Fig4.3 Basic elements of an artificial neuron	38
Fig4.4 Threshold activation function	39
Fig4.5 Piecewise-linear function	39
Fig4.6 Sigmoid (logistic) function	39
Fig4.7 Hyperbolic tangent function	39
Fig4.8 Schematic presentation of weight correction in BPNN	43
Fig4.9 Back propagation algorithm	43
Fig4.10 Optimal NN selection process	47
Fig4.11 Flowchart of optimal NN selection	48
Fig5.1 Experimental results graphic of NN model 1	52
Fig5.2 Experimental results graphic of NN model 2	53
Fig5.3 Main Effects Plot for NN model 1	56
Fig5.4 Main Effects Plot for NN model 2	56
Fig5.5 2D Parametric Study for NN model 1	57
Fig5.6 2D Parametric Study for NN model 2	58
Fig5.7 3D Parametric Study for NN model 1	60
Fig5.8 3D Parametric Study for NN model 2	64

LIST OF SYMBOLS

A	: total area
A_o	: gross area enclosed by the shear flow path
A_e	: area enclosed by lines connecting the centroids of the reinforcing bars at the corner of the section
A_k	: area enclosed by the centre-lines of the effective wall thickness
A_ℓ	: total area of longitudinal torsional reinforcement
A_{sh}	: area enclosed by the centre of stirrups
A_{sv}	: area of the two legs of stirrups at a section ($=2A_t$)
A_t	: cross sectional area of one-leg of closed stirrup
a_i	: outputs of neural network
f_c	: compressive strength of concrete
$f_{y\ell}$: yield strength of longitudinal torsional reinforcement
f_{yv}	: yield strength of closed stirrups
k	: number of samples in training or test data
m	: number of segments in training or test data
n	: number of outputs of neural network for training and test procedures
ρ_ℓ	: steel ratio of longitudinal reinforcement
ρ_t	: steel ratio of stirrups
p_h	: perimeter of centerline of outmost closed transverse torsional reinforcement
R^2	: correlation coefficient
s	: spacing of stirrups
s_x	: normalized value of variable
T_c	: torsion moment resisted by the concrete compression struts
T_n	: nominal torsional strength
$T_{u(\text{estimated})}$: predicted ultimate torsional strength
$T_{u(\text{experimental})}$: measured ultimate torsional strength
t_{ef}	: the effective wall thickness
t_i	: desired outputs
u	: perimeter of the cross-section
x	: short dimension of the cross section
y	: long dimension of the cross section
x_1	: center-to-center of the shorter and longer legs of stirrups
y_1	: center-to-center of the longer legs of stirrups
Z	: variable values
Z_{min}	: variable minimum values
Z_{max}	: variable maximum values
θ	: angle of compression diagonals

CHAPTER 1

INTRODUCTION

1.1 General Introduction

There are many variables affecting the torsional strength of RC beams such as cross-sectional area of beams, dimensions of closed stirrup, spacing of stirrups, cross-sectional area of one-leg of closed stirrup, yield strength of stirrup and longitudinal reinforcement and concrete compressive strength. The effect of these variables on the torsional strength of RC beams has been extensively studied and some empirical approach has been developed related to variables. For instance, Victor and Muthukrishnan (1973) studied the effect of variations in stirrups on the torsional capacity of RC beams and they proposed an empirical relationship for the contribution by stirrups to torsional capacity. Rasmussen and Baker (1995) examined the behavior of reinforced normal concrete and high strength concrete beams subjected to pure torsion.

The test have showed that high strength concrete increase the beam torsional capacity and stiffness. McMullen and Rangan (1978) presented the results of torsion test on rectangular RC beams with the aspects ratio and amount reinforcement as main variables. The effect of high strength concrete on the torsional behavior of RC beams under pure tension was investigated by Koutchoukali and Belarbi (2001) and Fang and Shiau (2004). According to the research the torsional capacity of under – reinforced beams is independent of concrete strength. They also found that the amount of longitudinal reinforcement was more effective in controlling crack width than the amount of transverse reinforcement. The torsional behavior of normal strength concrete beams has also been reported by other researchers.

Test data are often used for validation, calibration or even development of models. Even though the torsional strength of RC beams has been carefully examined experimentally, estimation of torsional strength is still difficult task because of complex behavior of RC beam under torsional action.

The general aims of this study is to investigate the usability of artificial neural network (ANN) models in predicting the torsional strength of RC beams and to evaluate the accuracy of the building codes in predicting the ultimate torsional strength of RC beams. To achieve these objectives, experimental data of 76 beams subjected to torsion were used from the existing database of Rasmussen and Baker (1995), Koutchoukali and Belarbi (2001), Fang and Shiau (2004), (Hsu ,1968) . By using their experimental results, the 12 different back-propagation algorithms were performed for the training of torsional strength of RC beams. Training error, test error, training time and correlation coefficient (R^2) that indicates the initial performance evaluation of different back propagation, were also compared for each of the 12 ANN algorithms. In addition to these, some building code' approaches as ACI-318-2005 (2005), Eurocode-2 (2002), TBC-500-2000 (2000), CSA (1994), BS8110 (1985) and AS3600 (2001) are also examined by comparing their predictions with mentioned experimental studies results. The results obtained by ANNs and building codes are compared with each other.

1.2 Layout of the Thesis

The layout of the thesis is described below:

- A literature survey for torsional strength of reinforced concrete beams and artificial neural networks are summarized in the next chapter.
- Chapter 3 is devoted to the torsional strength of RC beams. The basic theory and torsional strength formula of RC beams presented and several Building Codes examples are studied.
- Chapter 4 is presents history, element and classification of artificial neural network. Back propagation algorithm, MATLAB NN Toolbox and optimal NN model selection are summarized.

- Chapter 5 deals with statistical parameters of testing and training sets and overall results of NN models and experimental results 2D and 3D graphics of NN models.
- Finally in Chapter 6 brief conclusions are presented together with some suggestions for future works.

CHAPTER 2

LITERATURE REVIEW

2.1 Engineering Analysis

Engineering analysis is the process of taking given "input" information defining the physical situation at hand and, through an appropriate set of manipulations, converting that input into a different form of information, the "output," which provides the answer to some questions of interest (Gallegher, 1995). The purpose of any engineering analysis is to predict the behavior of an engineering system under specified conditions. In other words: given the input to the system what is the output from the system? The engineering system under analysis could be, for example, a simple elastic beam, a complex nonlinear three-dimensional structure, mechanical equipment or a hydraulic network

Irrespective of what the engineering system (the physical system) is, it *is*, first converted into a mathematical model and the mathematical model is then analyzed to predict its behavior whether the mathematical model is a simple one or a complex one and whether the analysis is a simple hand calculation or an elaborate computerized analysis, results of the analysis will always have a certain amount of uncertainty associated with it. Uncertainties arise because of the approximations and assumptions made in the conversion of the physical system to a mathematical model in the analysis procedure. Traditionally the uncertainty is not quantified but is recognized and accounted for in designs through safety factors (Ayyub, 1997).

2.2 RC Beams

Various approaches are available in the literature for the determination of the ultimate torsional strength of reinforced concrete beams. The space truss theory (Rausch,1929) is overconservative specially for underreinforced sections (Hsu, 1968) whereas the skew bending model (Lessig,1953); (Yudin,1962) appears to better predict the observed results, but is cumbersome to use and sometimes can be overconservative.

An interesting limit analysis method to find the ultimate torsional strength of reinforced concrete members was proposed by Wang and Hsu (1997), in which the work equation based upon the energy dissipation rate and the permissible failure mechanism at the ultimate state was used. This method gives good estimates of the experimental results reported by (Hsu ,1968).

Taking a clue from their earlier work Phatak and Dhonde (1999), the writers have formulated a general equation to determine the ultimate torsional strength of reinforced concrete beams using a unique method of dimensional analysis. The results predicted by dimensional analysis are then compared with the experimental results (Hsu ,1968) and the limit analysis method Wang and Hsu (1997).

2.2.1 Advantages of Using High Strength Concrete

There are many advantages of high strength concrete. The following list provides some of them.

- Reduction in member size, resulting in (a) increase in rentable space and (b) reduction in the volume of produced concrete with the accompanying saving in construction time.
- Reduction in the self-weight and superimposed dead load with the accompanying saving in smaller foundations.
- Reduction in formwork area and cost with the accompanying reduction in shoring and stripping time due to high early-age gain in strength.

- Construction of higher high-rise buildings with the accompanying saving in real estate costs in congested areas.
- Longer spans and fewer beams of the same magnitude of loading.
- Reduced axial shortening of compression supporting members.
- Reduction in the number of supports and the supporting foundations due to the increase in spans.
- Reduction in the thickness of floor slabs and supporting beam sections (a major component of the weight and cost of the majority of structures).
- Superior long-term service performance under static, dynamic, and fatigue loading.
- Low creep and shrinkage.
- Greater stiffness as a result of a higher modulus, E_c .
- Higher resistance to freezing and thawing, chemical attack, and significantly improved long-term durability and crack propagation.

2.3 Neural Networks

Over the past few years, interest in artificial neural networks has grown rapidly. Professionals from such diverse fields as engineering, philosophy, physiology, and psychology recognize the potential offered by this technology and are seeking applications within their disciplines. Recently, the artificial neural network has experienced a surge in popularity and is now one of the most rapidly expanding areas of research across many disciplines. The main reason is in its powerful and adaptive abilities to treat various complex problems. One can be sure that with its further developments, neural networks will strongly impact many conventional disciplines from the standpoint of methodology. In the field of mechanics, the research and application of both neural network and revolutionary computing are especially active and successful. The back propagated multilayered network is one of the main types applied to engineering (Zeng,1998).

2.3.1 Neural Networks in Structural Mechanics

The application of NNs in structural mechanics has been gaining support in the recent years. The NN models adopted for structural mechanics may have different architectures and may possess different patterns of connectivity. NNs have been used as computational tools in various areas of structural mechanics, amongst them, identification, simulation, assessment, optimization, analysis and design. The range of applications of Backpropagation neural networks in computational structural mechanics may include design, optimization, identification, mesh generation and analysis (Topping and Bahreininejad, 1997).

One of the major tasks in NN studies is obviously the determination of the optimum NN architecture which is based on trial and error processes. This is the most difficult and time consuming part of the study. However, there is no well established study in the fields of structural analysis by NNs covering the automatic selection of the optimum NN architecture. This will save much more time and simplify NN applications to a great extent.

CHAPTER 3

THEORY OF TORSIONAL STRENGTH OF REINFORCED CONCRATE BEAMS

3.1 Torsional Strength

3.1.1 Theories of Torsional Strength and Torsion in the Building Standards

The method for analysis of torsional strength can be roughly classified into two main categories: the skew-bending and the space-truss analogy theory. In this section, the two theories for torsional strength of reinforced concrete members are reviewed briefly. On the other hand, the ACI Building Code provisions for torsional design were selected and used in this study for comparison with the results from the RBFN models. Therefore, the ACI equations for torsional strength of RC beams are also outlined in the following.

In the space truss model the torsion is resisted by compression diagonals that consist of the concrete between cracks that spiral around the beam at a constant angle. The theory has been extended later by many scholars in this field (Hsu,1968), Elfegren et al.(1974). It is assumed in this theory that the concrete beam behaves in torsion similar to a thin-walled box with a constant shear flow in the wall cross-section, producing a constant torsional moment (Nawy,2003). The absence of core does not affect the strength of such members in torsion; hence the acceptability of the space truss analogy approach based on hollow sections. Therefore, in the process of torsion design of a RC beam, the beam can be considered to be equivalent tubular member Çevik et al.(2010).

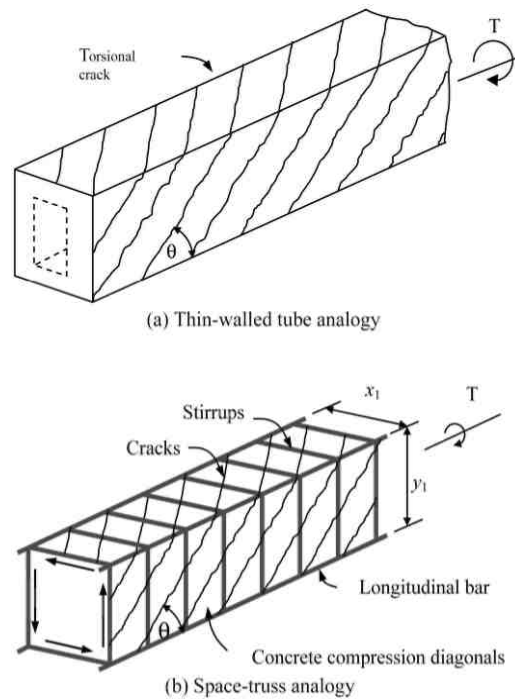


Fig3.1 Thin-walled tube and space-truss analogy (Tang, 2006)

In 1958, the skew-bending theory which considers in detail the internal deformational behavior of the series of transverse warped surfaces along the beam was proposed by (Lessig,1959). The model was further refined by Collins et al.(1965) in 1965 as well as Hsu and Zia (Hsu,19689,Zia and Hsu (2004). Especially Hsu made a major contribution experimentally to the development of the skew-bending theory as it presently stands. The basic approach of the theory is that the failure of a rectangular section in torsion occurs by bending about an axis which is parallel to wider face of the section and inclined at about 45° to the longitudinal axis of the beam. In previous versions of ACI code (from 1971 to 1989) (ACI Committee), torsional strength of beams was calculated by using this theory. According to the codes, torsional strength T_n of beams was considered to be made up of two parts: one part is contributed by concrete T_c while the other part is contributed by web reinforcement T_s .

Hsu (Hsu,1968) on hollow and solid rectangular beams, it was observed that the concrete core does not contribute to the ultimate torsional strength. Later he concluded that the concrete contribution T_c was mainly due to the shear resistance of the diagonal concrete struts

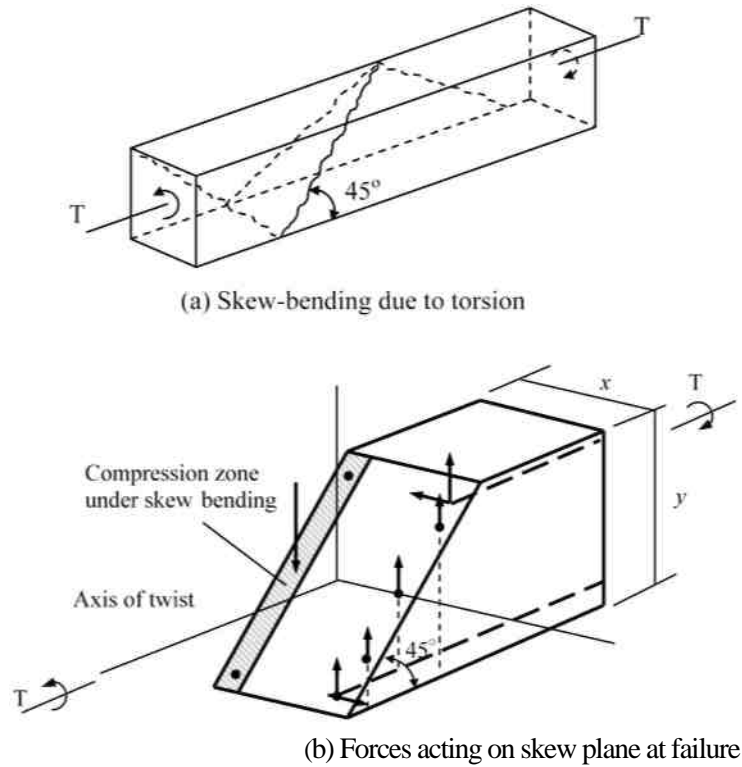


Fig3.2 Skew-bending theory analogy (Tang, 2006)

ACI code (1995) was proposed a radically different design procedure based on the thin-walled tube, space truss analogy which is considerably simpler to understand and apply and is equally accurate. The torsion provisions in the ACI 318 have been revised using the thin walled tube analogy (ACT ,1999).

According to the current torsion provision of ACI 318-2005 (2005), meaningful additional torsional strength T_n of RC beams can be achieved only by using both closed stirrups and longitudinal steel bars while the torsion moment T_c resisted by the concrete compression struts is assumed as zero.

Thus the concrete contribution is ignored; there is no advantage in using higher concrete strengths in resisting ultimate torsion. The torsional strength T_n is given as follows;

$$T_n = \frac{2A_o A_t f_{yv}}{s} \cot \theta \quad (3.1)$$

In the Eq.1, $\cot \theta$ can be assumed as

$$\cot \theta = \sqrt{\frac{A_{\ell} f_{y\ell} s}{A_t f_{yv} p_h}} \quad (3.2)$$

In the equation 1 and 2, A_o is the gross area enclosed by the shear flow path that can be equal to $0.85 A_{sh}$, where A_{sh} is the area enclosed by the centre of stirrups. θ angle of compression diagonals, $f_{y\ell}$ yield strength of longitudinal torsional reinforcement, f_{yv} is yield strength of closed stirrups, A_{ℓ} total area of longitudinal torsional reinforcement, p_h perimeter of centerline of outmost closed transverse torsional reinforcement, s spacing of stirrups, A_t cross sectional area of one-leg of closed stirrup Çevik et al.(2010).

In Australian Standard AS3600 (2001) and Canadian Standard CSA,(1994) the design of RC beams subjected to pure torsion is based on the space truss model and the T_n value is given as the same equation with ACI-318-2005 (2002). Different from ACI 318-2005 (1995), CSA (1994) and AS3600 (2001), The British Standards BS8110 (1985) for RC structures, the torsional strength shall be calculated from Equation 3 as;

$$T_n = \frac{0.8x_1y_1(0.87f_{ys})A_{sv}}{s} \quad (3.3)$$

where A_{sv} is the area of the two legs of stirrups at a section and x_1 and y_1 are the center-to-center of the shorter and longer legs of stirrups given in Figure 3.1. The torsional strength T_n is described as Equation 4 in Turkish Building Code TBC-500-2000.

$$T_n = \frac{2A_{\ell}A_e f_{yv}}{2(x_1 + y_1)} \quad (3.4)$$

In the Equation 4, A_e is area enclosed by lines connecting the centroids of the reinforcing bars at the corner of the section as seen in Figure 3.3.

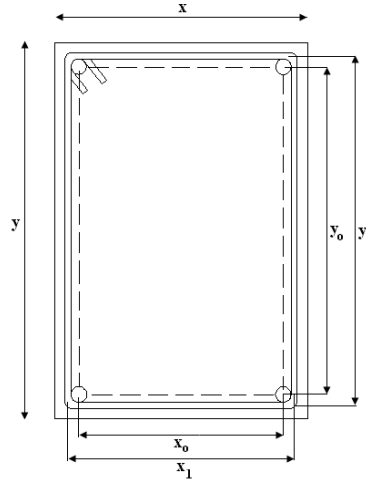


Fig3. 3 The cross section of a rectangular reinforced concrete beam
Çevik et al.(2010).

According to the European Standard Eurocode-2 (2002), torsional strength shall be calculated with three ways and the minimum result is chosen.

$$T_n = f_{ys} (A_{sw} / s) 2A_k \cot \theta \quad (3.5)$$

$$T_n = f_y (A_s / u_k) 2A_k \tan \theta \quad (3.6)$$

$$T_n = 1.2(1 - f_c / 250) f_c A_k t_{ef} \sin \theta \cos \theta \quad (3.7)$$

Where A_k is the area enclosed by the centre-lines of the effective wall thickness. The effective wall thickness, t_{ef} can be calculated as A/u where A is the total area and u is the perimeter of the cross-section, f_c is the compressive strength of concrete Çevik et al.(2010).

3.1.2 Pure Torsion in Concrete Elements

An introduction to the subject of torsional stress distribution has to start with the basic elastic behavior of simple sections, such as circular or rectangular sections. Most concrete beams subjected to twist are components of rectangles. They are usually flanged sections such as T beams and L beams.

Although circular sections are rarely a consideration in normal concrete construction, a brief discussion of torsion in circular sections serves as a good introduction to the torsional behavior of other types of sections. Shear stress is equal to shear strain times the shear modulus at the elastic level in circular sections. As in the case of flexure, the stress is proportional to its distance from the neutral axis and is maximum at the extreme fibers. When deformation takes place in the circular shaft, the axis of the circular cylinder is assumed to remain straight. All radii in a cross-section also remain straight and rotate through the same angle about the axis. As the circular element starts to behave plastically, the stress in the plastic outer ring becomes constant while the stress in the inner core remains elastic, as shown in Fig 3.4. (Nawy,2005).

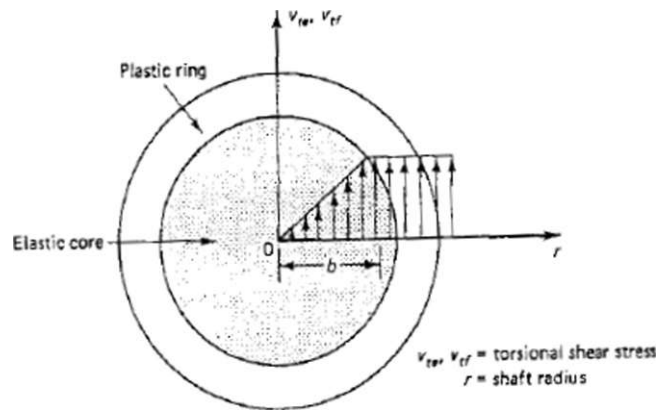


Fig3.4 Torsional stress distribution through circular section (Nawy,2005).

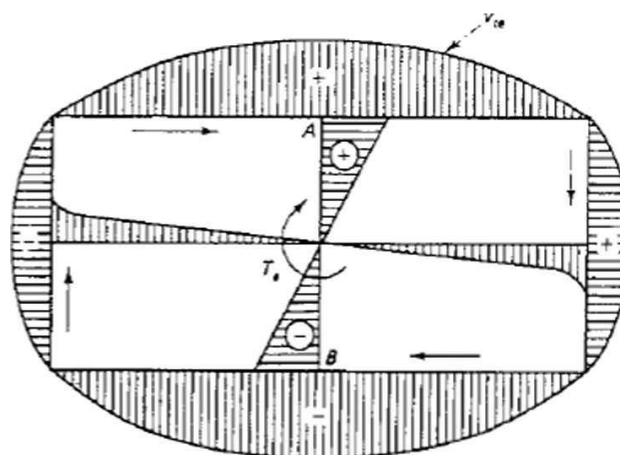


Fig3. 5 Pure torsion stress distribution in a rectangular section (Nawy,2005).

In rectangular sections, the torsional problem is considerably more complicated. The originally plane cross sections undergo warping due to the applied torsional moment, this moment produces axial as well as circumferential shear stresses with zero values at the corners of the section and the centroid of the rectangle and maximum values on the periphery at the middle of the sides, as seen in Figure 3.5. The maximum torsional shearing stress would occur at midpoints A and B of the larger dimension of the cross-section. These complications plus the fact that reinforced concrete sections are neither homogeneous nor isotropic make it difficult to develop exact mathematical formulations based on physical models (Nawy,2005).

For over sixty years, the torsional analysis of concrete members has been based on either (1) the classical theory of elasticity developed through mathematical formulations coupled with membrane analogy verifications (St. Venant's) or (2) the theory of plasticity represented by the sand-heap analogy (Nadai's). Both theories were applied essentially to the state of pure torsion. But experiments revealed that the elastic theory is not entirely satisfactory for the accurate prediction of the state of stress in concrete in pure torsion. The behavior of concrete was found to be better represented by the plastic approach. Consequently, almost all developments in torsion as applied to concrete and reinforced concrete have been in the latter direction (Nawy,2005).

3.1.3 Torsion in Elastic Materials

St. Venant presented in 1853 his solution to the elastic torsional problem with warping due to pure torsion that develops in noncircular sections. Prandl in 1903 demonstrated the physical significance of the mathematical formulations by his membrane analogy model. The model establishes particular relationships between the deflected surface of the loaded membrane and the distribution of torsional stresses in a bar subjected to twisting moments. Figure 3.6 shows the membrane analogy behavior for rectangular as well as L-shaped forms. For small deformations, it can be proved that the differential equation of the deflected membrane surface has the same form as the equation that determines the stress distribution over the cross-section of the bar subjected to twisting moments. Similarly, it can be demonstrated;

(1) the tangent to a contour line at any point of a deflected membrane gives the direction of the shearing stress at the corresponding cross-section of the actual member subjected to twist; (2) the maximum slope of the membrane at any point is proportional to the magnitude of shear stress at the corresponding point in the actual member; (3) the twisting moment to which the actual member is subjected is proportional to twice the volume under the deflected membrane. It can be seen from Fig3.3. that the torsional shearing stress is inversely proportional to the distance between the contour lines. The closer the lines are, the higher the stress, leading to the previously stated conclusion that the maximum torsional shearing stress occurs: it the middle of (he longer side of the rectangle. From the membrane analogy, this maximum stress has to be proportional to the steepest slope of the tangents at points *A* and *B* (Zhang,2002).

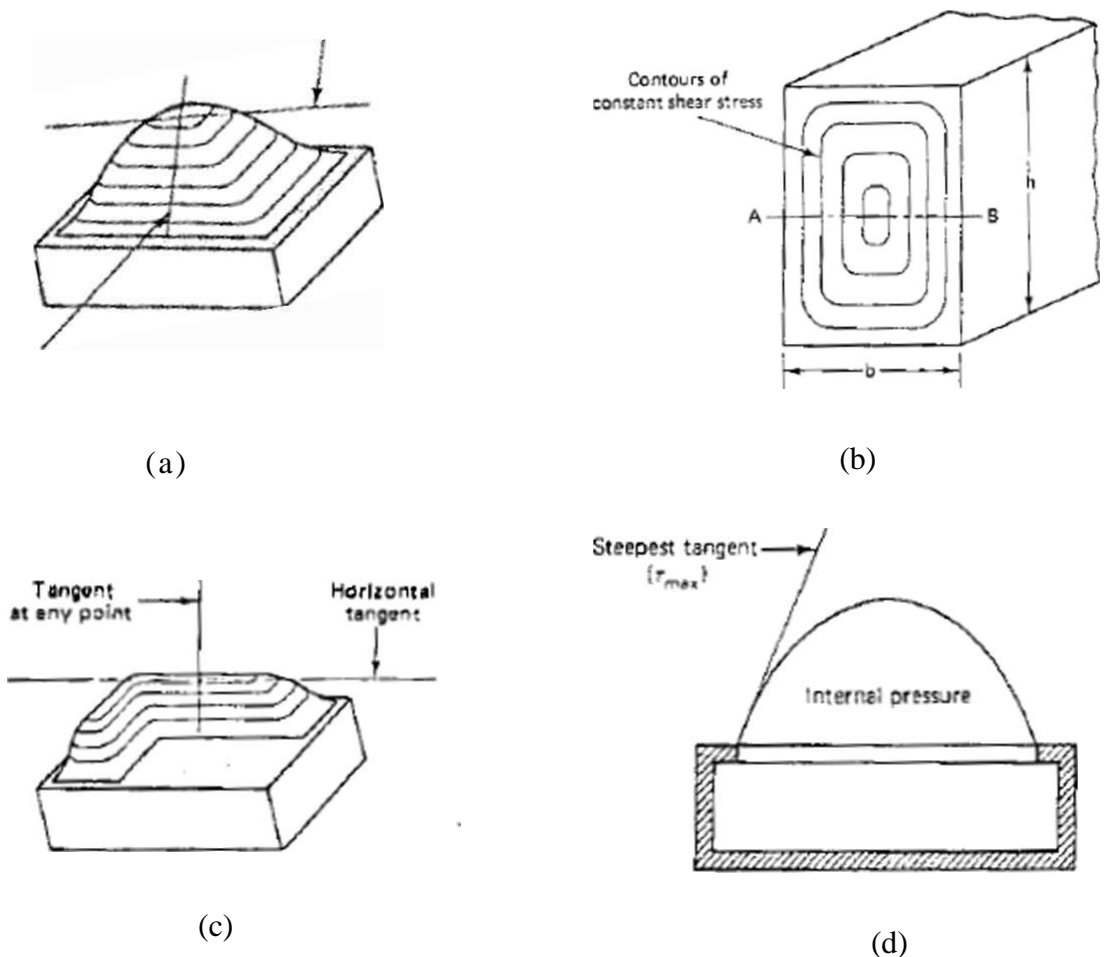


Fig3. 6 Membrane analogy in elastic pure torsion: (a) membrane under pressure; (b) contours in a real beam or in a membrane; (c) L-section; (d) rectangular section (Nawy,2005).

If δ = maximum displacement of the membrane from the tangent at point A, then

$$\delta = b^2 G \theta \quad (3.8)$$

from basic principles of mechanics and St. Venant's theory, (Nawy,2005).

where G is the shear modulus and θ is the angle of twist. But $V_{t(\max)}$ is proportional to the slope of tangent; hence (Nawy,2005).

$$V_{t(\max)} = k_1 b G \theta \quad (3.9)$$

where the k's are constants. The corresponding torsional moment T_ℓ is proportional to twice the volume under the membrane (Nawy,2005), or

$$T_\ell \propto 2 \left(\frac{2}{3} \delta b h \right) = k_2 \delta b h \quad (3.10)$$

or;

$$T_\ell = k_3 b^3 h G \theta \quad (3.11)$$

3.1.4 Torsion in Plastic Materials

As indicated earlier, the plastic sand-heap analogy provides a better representation of the behavior of brittle elements such as concrete beams subjected to pure torsion. The torsional moment is also proportional to twice the volume under the heap, and the maximum torsional shearing stress is proportional to the slope of the sand heap. Figure 3.7 is a two- and three-dimensional illustration of the sand heap.

The torsional moment T_p in Figure 3.7 d is proportional to twice the volume of the rectangular heap shown in parts (b) and (c). It can also be recognized that the slope of the sand-heap sides as a measure of the torsional shearing stress is constant in the sand-heap analogy approach, whereas it is continuously variable in the membrane analogy approach. This characteristic of the sand heap considerably simplifies the solutions (Zhang,2002).

3.1.5 Sand-heap Analogy Applied to L Beams

Most concrete elements subjected to torsion are flanged sections, most commonly L beams comprising the external wall beams of a structural floor. The L beam in Figure 3.8 is chosen in applying the plastic sand-heap approach to evaluate its torsional moment capacity and shear stresses to which it is subjected (Nawy, 2005).

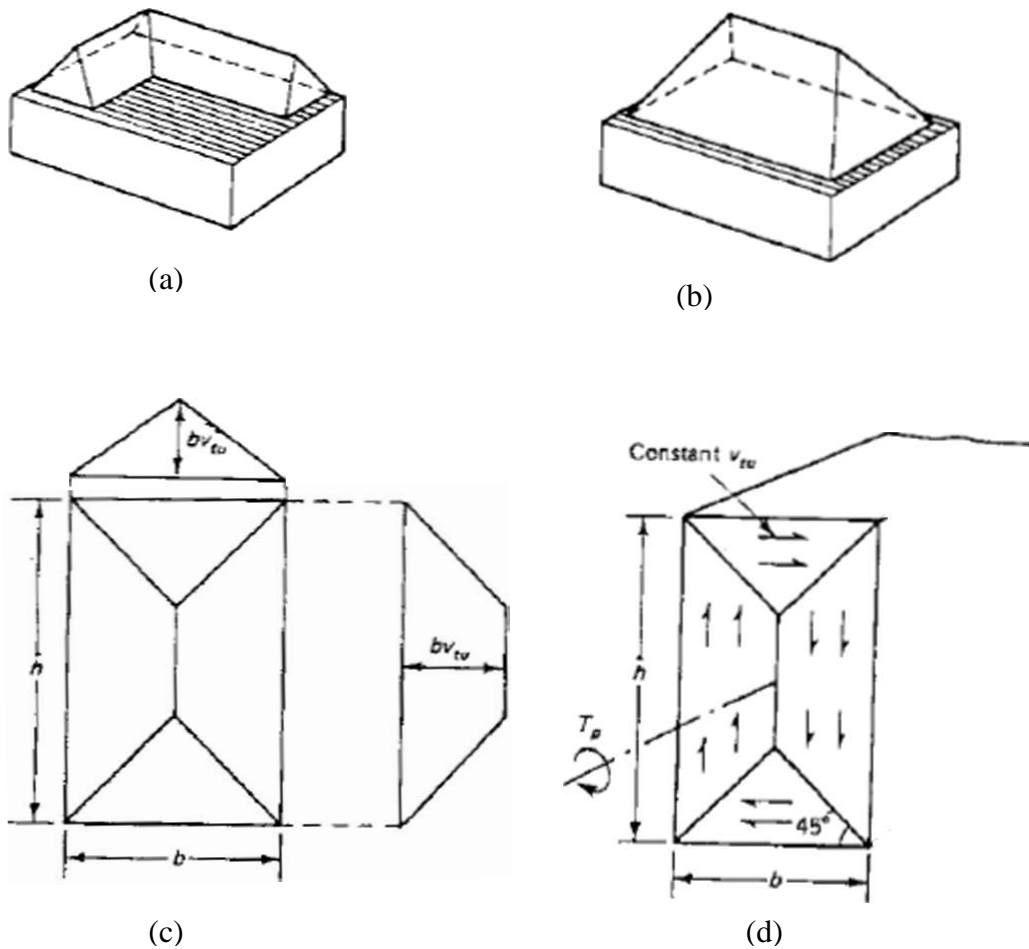


Fig3.7 Sand-heap analogy in plastic pure torsion: (a) sand-heap L-section (b) sand-heap rectangular section; (c) plan of rectangular section; (d) torsional shear stress (Nawy, 2005).

The sand heap is broken into three volumes:

$$V_1 = \text{pyramid representing a square cross-sectional shape} = y_1 b_w^2 / 3$$

$$V_2 = \text{tent portion of the web representing a rectangular cross-sectional shape} = y_1 b_w (h - b_w) / 2$$

$$V_3 = \text{tent representing the flange of the beam, transferring part PDI to NQM} = y_2 h_f (b - b_w) / 2$$

Torsional moment is proportional to twice the volume of the sand heaps; hence

$$T_p = 2 \left[\frac{y_1 b_w^2}{3} + \frac{y_1 b_w (h - b_w)}{2} + \frac{y_2 h_f (b - b_w) / 2}{2} \right] \quad (3.12)$$

Also, torsional shear stress is proportional to the slope of the sand heaps; hence

$$y_1 = \frac{v_t b_w}{2} \quad (3.12a)$$

$$y_2 = \frac{v_t h_f}{2} \quad (3.12b)$$

Substituting y_1 and y_2 from Eqs. 12a and 12b into Eq.12 gives us

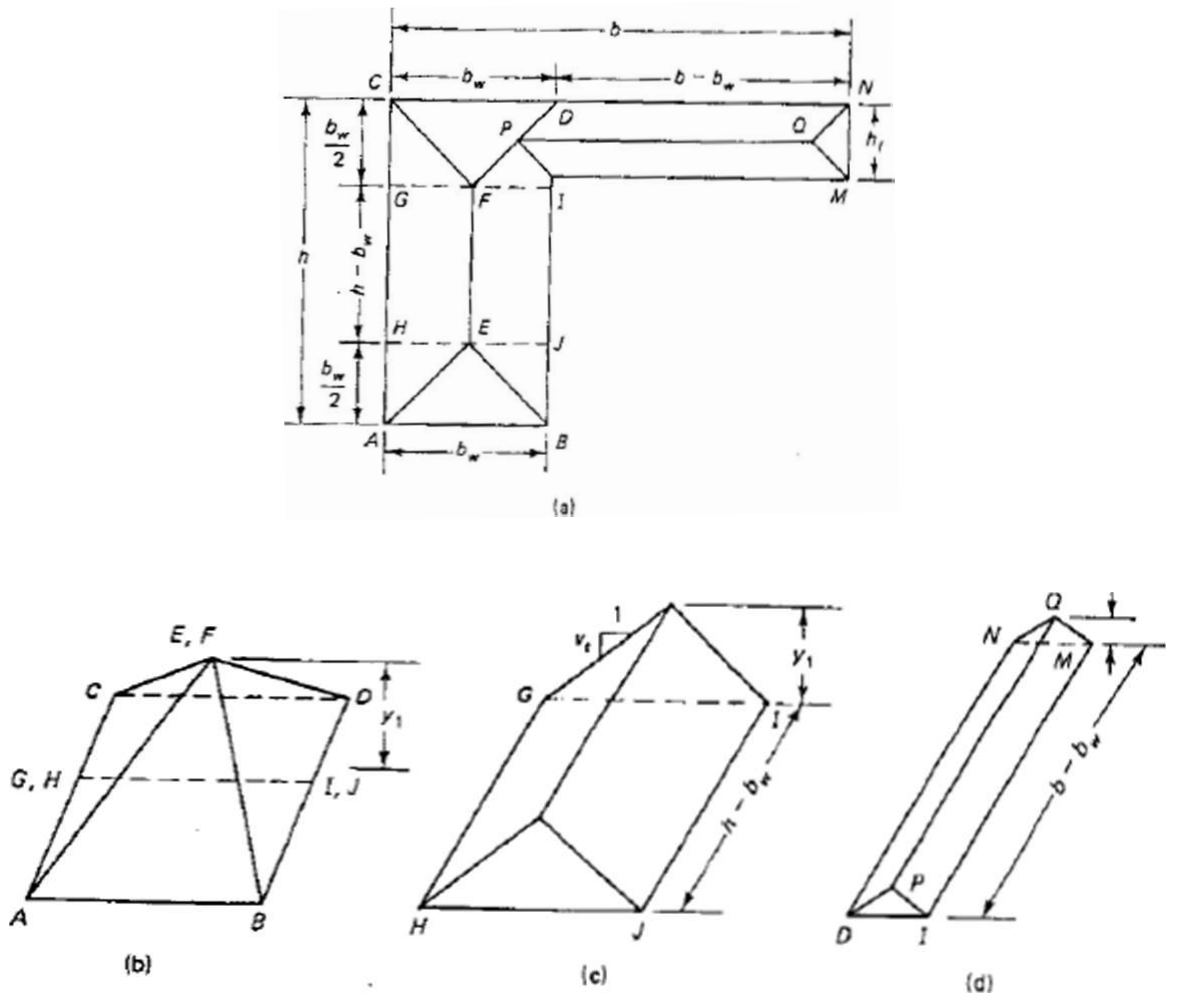


Fig3.8 Sand-heap analogy of flanged section: (a)sand heap on L-shaped cross section; (b)composite pyramid from web V_1 ; (c) tent segment from web V_2 ; (d) transformed tent of beam flange V_3 (Nawy,2005).

$$V_{t(\max)} = \frac{T_p}{(b_w^2 / 6)(3h - b_w) + (h_f^2 / 2)(b - b_w)} \quad (3.13)$$

If both the numerator and denominator of Eqn.13 are divided by $(b_w h)^2$ and the terms rearranged, we have ;

$$V_{t(\max)} = \frac{T_p h / (b_w h)^2}{\left[\frac{1}{6} (3 - b_w / h) \right] + \left[\frac{1}{2} (h_f / b_w) 2(b / h - b_w / h) \right]} \quad (3.14a)$$

If one assumes that C_1 is the denominator in Eqn.14a and $J_E = C_1 (b_w h)^2$ Eqn.14a becomes

$$V_{t(\max)} = \frac{T_p h}{J_E} \quad (3.14b)$$

where J_E is the equivalent polar moment of inertia and a function of the shape of the beam cross section. Note that Eqn.14b is similar in format to from the membrane analogy except for the different values of the denominator J and J_E . Eqn 14a can be readily applied to rectangular section by setting $h=0$ (Nawy,2005).

It must also be recognized that concrete is not a perfectly plastic material; hence the actual torsional strength of the plain concrete section has a value lying between the membrane analogy and the sand-hcap analogy values. Eqn 14b can be rewritten designating $T_p = T_c$ as the nominal torsional resistance of the plain concrete and $V_{t(\max)} = V_{tc}$ using ACI terminology, so that

$$T_c = k_2 b^2 h V_{tc} \quad (3.15a)$$

$$T_c = k_2 x^2 y V_{tc} \quad (3.15b)$$

where x is the smaller dimension of the rectangular section (Nawy,2005).

Extensive work by Hsu. confirmed by others, has established that k_2 , can be taken as $\frac{1}{3}$. This value originated from research in the skew-bending theory of plain concrete.

It was also established that $6\sqrt{f'_c}$ can be considered as a limiting value of the pure torsional strength of a member without torsional reinforcement (Nawy,2005).

Using a reduction factor of 2.5 for the first cracking torsional load $V_{tc} = 2.4\sqrt{f'_c}$ and using $k_2 = \frac{1}{3}$ in Eqn.15 results in

$$T_c = 0.8\sqrt{f'_c}x^2y \quad (3.16a)$$

where x is the shorter side of the rectangular section. The high reduction factor of 2.5 is used to offset any effect of shear and bending moments that might be present.

If the cross section is a T or L section, the area can be broken into component rectangles as in Figure3.9, (Nawy,2005) such that

$$T_c = 0.8\sqrt{f'_c} \sum x^2y \quad (3.16b)$$

3.1.6 Skew-Bending Theory

This theory considers in detail the internal deformational behavior of the series of transverse warped surfaces along the beam. Initially proposed by Lessig. it had subsequent contributions from Collins, Hsu, Zia. Gesund. Mattock, and Elfgren among the several researchers in this field. T. T. C. Hsu made a major contribution experimentally to the development of the skew-bending theory as it presently stands. Hsu details the development of the theory of torsion as applied to concrete structures and how the skew-bending theory formed the basis of the 1989 ACI Code provisions on torsion. The complexity of the torsional problem can thus permit in this textbook only the brief discussion that follows Collins and Mitchell, (1980).

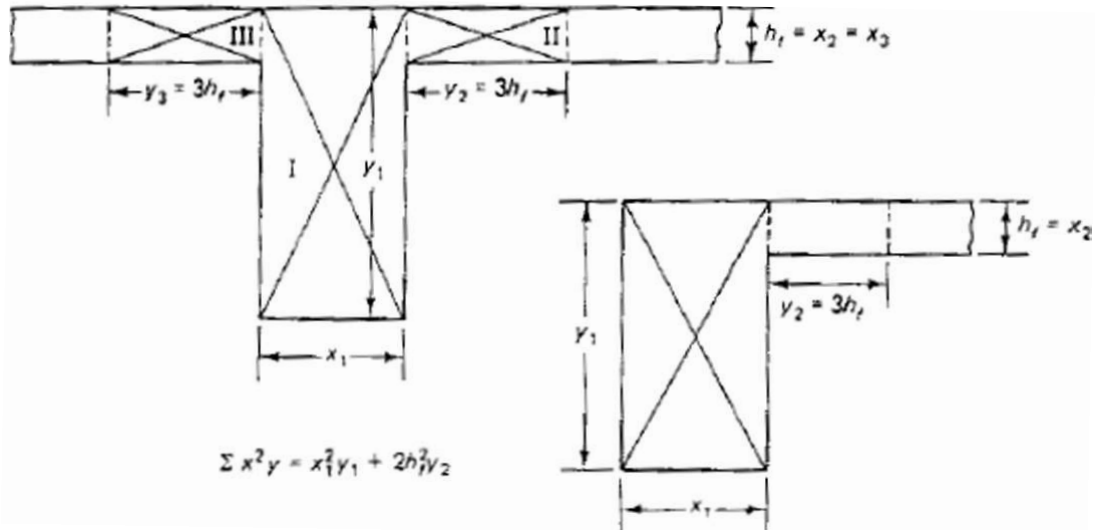


Fig.3.9 Component rectangles for T_c calculation (Nawy,2005).

The failure surface of the normal beam cross section subjected to bending moment M_u remains plane after bending, as in Figure 3.10a. If a twisting moment T_u is also applied exceeding the capacity of the section, cracks develop on three sides of the beam cross-section and compressive stresses on portions of the fourth side along the beam. As torsional loading proceeds to the limit state at failure, a skewed failure surface results due to the combined torsional moment T_u and bending moment M_u . The neutral axis of the skewed surface and the shaded area in Figure 1.10b denoting the compression zone would no longer be straight but subtend a varying angle θ with the original plane cross-sections (Nawy,2005).

Prior to cracking, neither the longitudinal bars nor the closed stirrups make any appreciable contribution to the torsional stiffness of the section. At the post-cracking stage of loading, the stiffness of the section is reduced, but its torsional resistance is considerably increased, depending on the amount and distribution of both the longitudinal bars and the transverse closed ties. It has to be emphasized that little additional torsional strength can be achieved beyond the capacity of the plain concrete in the beam unless both longitudinal torsion bars and transverse ties are used.

The skew-bending theory idealizes the compression zone by considering it to be of uniform depth. It assumes the cracks on the remaining three faces of the cross section to be uniformly spread, with the steel ties (stirrups) at those faces carrying the tensile forces all the cracks and the longitudinal bars resisting shear through dowel action with the concrete. Figure 3.11a shows the forces acting on the skewlv bent plane (Nawy,2005).

The polygon in Figure 1.11b gives the shear resistance F_c of the concrete, the force T_r of the active longitudinal steel bars in the compression zone, and the normal compressive block force C_u .

The torsional moment T_c of the resisting shearing force F_c generated by the shaded compressive block area in Figure 3.11a is thus

$$T_c = \frac{F_c}{\cos 45^\circ} \times \text{its arm about forces } F_v \text{ in Fig3.11a}$$

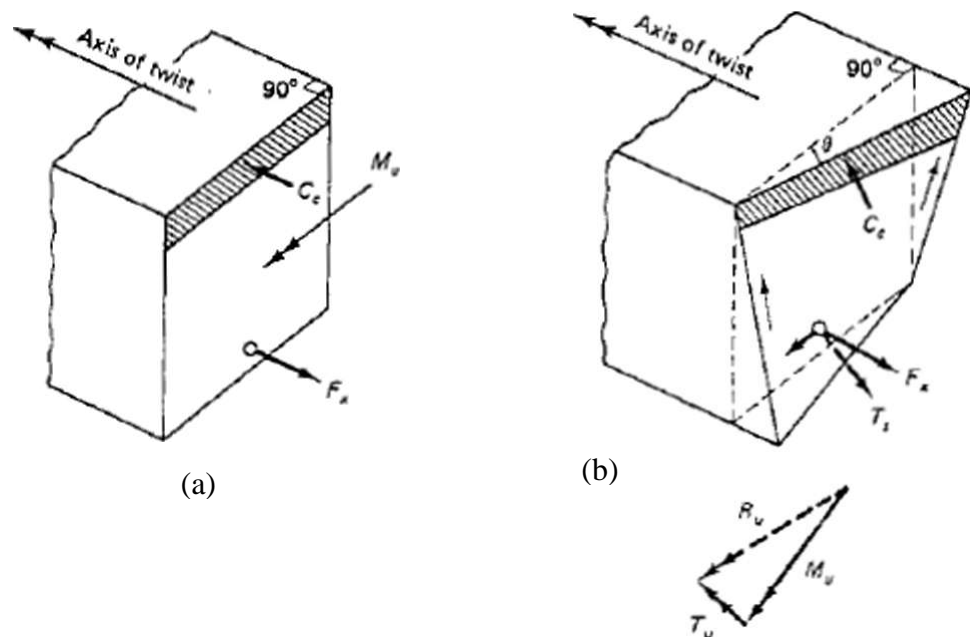


Fig3.10 Skew bending due to torsion: (a) bending before twist; (b) bending and torsion (Nawy,2005).

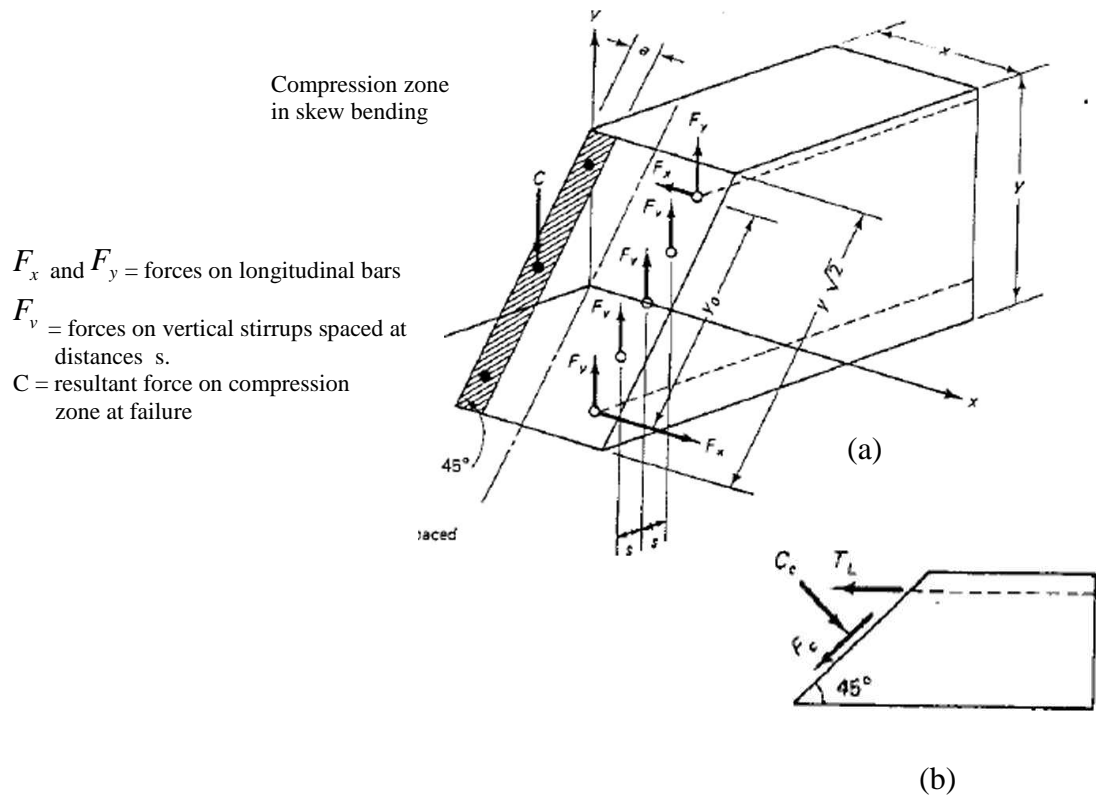


Fig 3.11. Forces on the skewly bent planes: (a) all forces acting on skew plane at failure; (b) vector forces on compression zone Nilson and Winter,(1991).

$$T_c = \sqrt{2}F_c(0.8x) \quad (3.17a)$$

where x is the shorter side of the beam. Extensive tests to evaluate F_c in terms of internal stress in concrete $k_1\sqrt{f'_c}$ and the geometrical torsional constants of the section k_2x^2y led to the expression (Nawy,2005).

$$T_c = \frac{2.4}{\sqrt{x}} x^2 y \sqrt{f'_c} \quad (3.17b)$$

3.1.7 Torsion In Reinforced Concrete Elements

Torsion rarely occurs in concrete structures without being accompanied by bending and shear. The foregoing should give a sufficient background on the contribution of the plain concrete in the section toward resisting part of the combined stresses resulting from torsional, axial, shear, or flexural forces. The capacity of the plain concrete to resist torsion when in combination with other loads could, in many cases, be lower than when it resists the same isolated external twisting moments alone. Consequently, torsional reinforcement has to be provided to resist the excess torque (Nawy,2005).

Inclusion of longitudinal and transverse reinforcement to resist part of the torsional moments introduces a new element in the set of forces and moments in the section.

T_n = required total nominal torsional resistance of the section including the reinforcement

T_c = nominal torsional resistance of the plain concrete

T_x = torsional resistance of the reinforcement

Then ;

$$T_n = T_c + T_x \quad (3.18)$$

T_c is assumed equal to zero for design simplification, and all the torsion is assumed to be borne by the longitudinal steel bars and the closed transverse stirrups. To study the contribution of the longitudinal steel bars and the closed stirrups, one has to analyze the system of forces acting on the warped cross-sections of the structural element at the limit state of failure. A modified space truss analogy is presented comparable to the plane truss analogy used for the design of shear stirrups. In this theory, both the longitudinal reinforcement and the transverse stirrups (ties) are utilized as components of the space truss (Nawy,2000).

3.1.8 Space Truss Analogy Theory

This theory was originally developed by Rausch and extended later by Lampert and Collins, with additional work by Hsu, Thurliman, Elfgren, and others. Further refinement was introduced by Collins and Mitchell (Hsu,1983) as a compression field theory.

(Hsu,1983) proposed combining the equilibrium, compatibility, and the softened constitutive laws of concrete in a unified theory that can predict with reasonable accuracy the shear and torsional behavior of beams (the softened truss model). The shear flow concept is utilized in deriving the relevant expressions for shear equilibrium.

The space truss analogy is an extension of the model used in the design of the shear resisting stirrups, in which the diagonal tension cracks, once they start to develop, are resisted by the stirrups. Because of the nonplanar shape of the cross-sections due to the twisting moment, a space truss composed of the stirrups is used as the diagonal tension members, and the idealized concrete strips at a variable angle between the cracks are used as the compression members, as shown in Figure3.12. (Nawy,2005).

It is assumed in this theory that the concrete beam behaves in torsion similar to a thin-walled box with a constant shear flow in the wall cross-section, producing a constant torsional moment. The use of hollow-walled sections rather than solid sections proved to give essentially the same ultimate torsional moment, provided that the walls are not too thin. Such a conclusion is borne out by tests, which have shown that the torsional strength of the solid sections is composed of the resistance of the closed stirrup cage, consisting of the longitudinal bars and transverse stirrups, and the idealized concrete inclined compression struts in the plane of the cage wall. The compression struts are the inclined concrete strips between the cracks in Figure 3.12. (Hassoun,1985).

The CFB-FIP code is based on the space truss model. In this code, the effective wall thickness of the hollow beam is taken as $\frac{1}{6}D_a$ where D_a is the diameter of the circle inscribed in the rectangle connecting the corner longitudinal bars; that is $D_0 = x_a$ in Figure 3.12. (Nawy,2005).

A rational method to derive the effective wall thickness was given by Hsu (Nawy,2000). This nonlinear analysis takes into account the warping compatibility condition of the wall. In summary, the absence of the core does not affect the strength of such members in torsion: hence the acceptability of the space truss analogy approach based on hollow box.

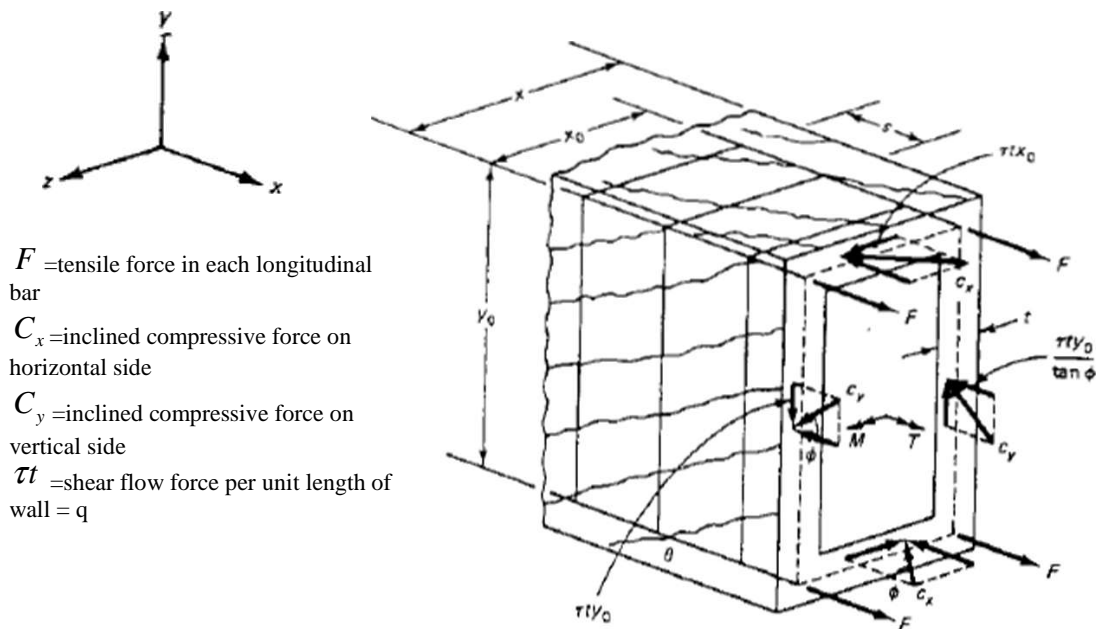


Fig3.12 Forces on hollow box concrete surface by truss analogy (Nawy,2005).

3.1.9 Equilibrium in Element Shear

A unit square membrane element of thickness h is subjected to shear flow q due to pure shear as in Figure 3.13 (Nawy,2000). Reinforcement in both the longitudinal (E-W) direction ℓ and transverse (N-S) direction t is subjected to a unit stress f_ℓ / s_ℓ and f_t / s_t respectively such that the shear flow q can be defined by the equilibrium equations

$$q = F_\ell \tan \theta \quad (3.19a)$$

where unit $F_\ell = A_\ell f_\ell / s_t$ and ;

$$q = F_t \cot \theta \quad (3.19b)$$

where unit $F_t = A_t f_t / s$, A is the cross-sectional area of the reinforcement, s_ℓ and s are the spacings in the t and ℓ directions, respectively.

From the geometry of the triangles in Figure 3.13, the shear flow can also be defined as;

$$q = (f_D t) \sin \theta \cos \theta \quad (3.19c)$$

If the reinforcement in both directions is assumed to have yielded. Eqn. 19a and b give

$$\tan \theta = \sqrt{\frac{F_{ty}}{F_{\ell y}}} \quad (3.20a)$$

and
$$q_y = \sqrt{F_{\ell y} F_{ty}} \quad (3.20b)$$

where the subscript y denotes the yielding of reinforcement.

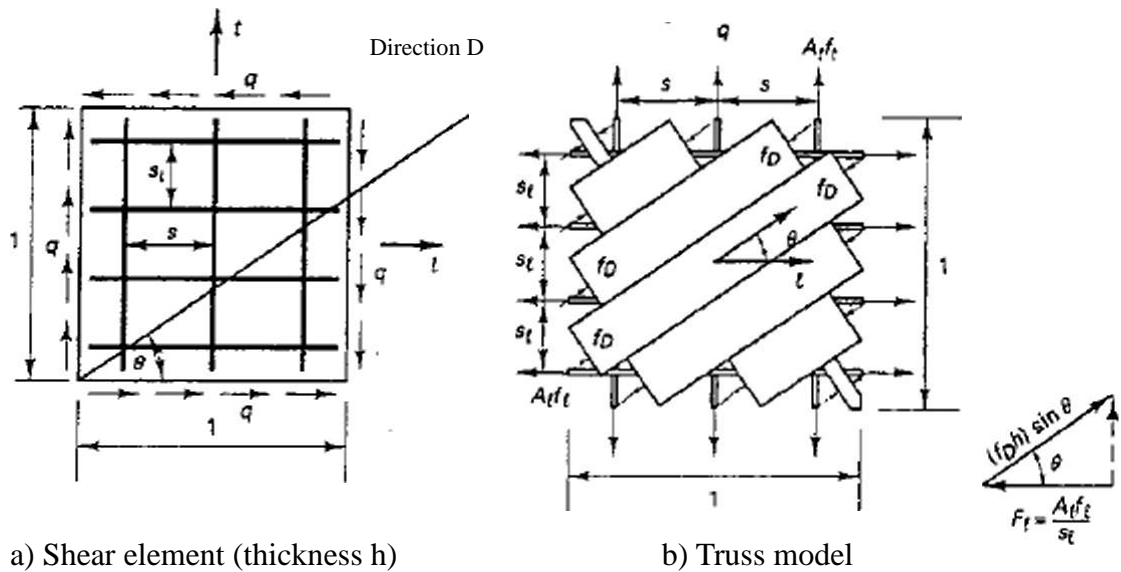


Fig3.13 Equilibrium forces in element shear (Nawy,2000).

3.1.10 Equilibrium in Element Torsion

The case of a hollow tube of any shape and variable thickness is considered Figure 3.14. It is subjected to pure torsion. St. Venant's theory stipulates that the cross-sectional shape remains unchanged in elastic small deformations, and the warping deformation perpendicular to the cross-section would be the same along the member's axis. Hence it can be assumed that only shear stresses develop in the tube wall in the form of shear flow q in Figure 3.14a and that the in-plane normal stresses in the wall vanish (Nawy, 2005). If an infinitesimal wall element ABCD is isolated as in Figure 3.14b the shear flow in the ℓ direction has to be equal to the shear flow in the t direction or

$$\tau_1 t_1 = \tau_2 t_2 \quad (3.21)$$

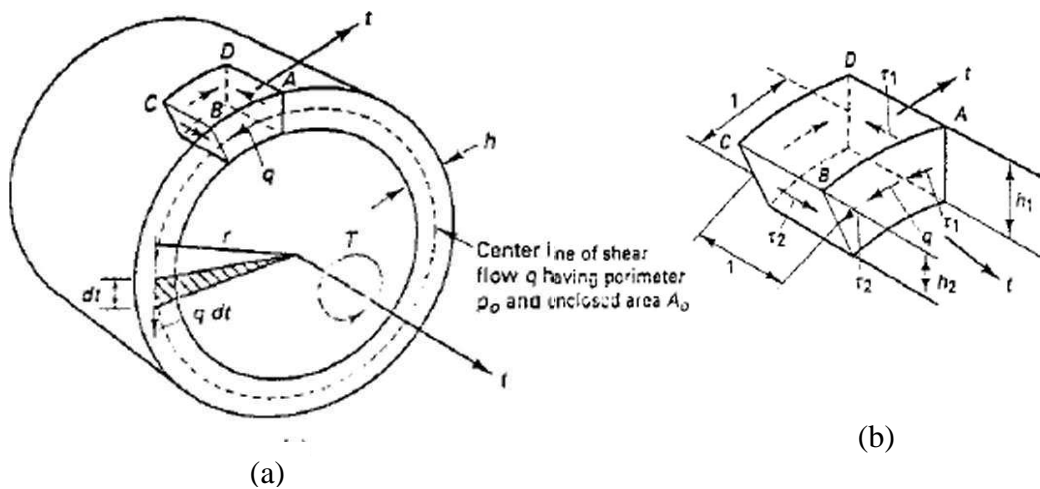


Fig3.14 Hollow tube equilibrium torsion forces: (a) section of tube subjected to torsion T ; (b) unit shear element from tube wall of varying thickness h , Note: ℓ and t denote the longitudinal and transverse directions, respectively (Nawy, 2005).

3.1.11 Shear-Torsion-Bending Interaction

Consider the rectangular boxes in Figures 3.13. The shear flow q will not be the same on the four walls of the box when subjected to combined shear and torsion. Failure can precipitate in two distinct modes:

- (a) Yielding of the longitudinal bottom tension steel and the transverse stirrups
- (b) Yielding of the longitudinal top compression steel and the transverse stirrups

(a) Bottom tension steel yielding. If the failure mode is caused by yielding of the longitudinal bottom stringer (tensile steel) and the transverse stirrups due to combined shear and torsion, the following expression can be derived from equilibrium (Nawy,2000).

$$\frac{M}{F_B y_0} + \left(\frac{V}{2y_0} \right)^2 \frac{y_0}{F_B} \frac{s}{Af_{yt}} + \left(\frac{T}{2A_0} \right)^2 \frac{y_0 + x_0}{F_B} \frac{s}{Af_{yt}} = 1 \quad (3.22)$$

If M_0 , V_0 and T_0 are the moments and forces acting alone they can be defined as follows:

$$M_0 = F_B y_0 \quad (3.23a)$$

$$V_0 = 2y_0 \sqrt{\frac{F_T A f_v}{y_0 s}} \quad (3.23b) \quad \text{for a two web box.}$$

$$T_0 = 2A_0 \sqrt{\frac{2F_T A f_v}{p_0 s}} \quad (3.23c)$$

where $p_0 = 2(y_0 + x_0)$

$$R = \frac{F_T}{F_B} \quad (3.23d)$$

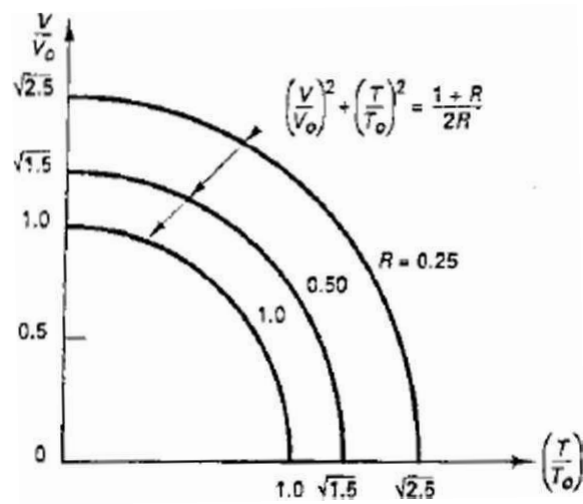


Fig3.15 Shear-torsion interaction diagram (Nawy,2005).

A nondimensional interaction surface relationship can be obtained by introducing Eqn3.23 into Eqn3.22 such that

$$\left(\frac{M}{M_0}\right) + \left(\frac{V}{V_0}\right)^2 R + \left(\frac{T}{T_0}\right)^2 R = 1 \quad (3.24a)$$

(b) Top compression steel yielding. If the failure mode is caused by yielding of the longitudinal top chord (compression steel) and the transverse stirrups, Eqn. 24a becomes

$$-\left(\frac{M}{M_0}\right) \frac{1}{R} + \left(\frac{V}{V_0}\right)^2 + \left(\frac{T}{T_0}\right)^2 = 1 \quad (3.24b)$$

From both Eqn 24a and b the interaction of V and T is circular for a constant bending moment M for both failure surfaces. The intersection of the two failure surfaces for these two failure modes forms a peak interaction curve between V and T such that Eqn 24a and b give

$$\left(\frac{V}{V_0}\right)^2 + \left(\frac{T}{T_0}\right)^2 = \frac{1+R}{2R} \quad (3.25a)$$

Equation 25a for $R = 0.25, 0.5$ and 1.0 on the peak planes gives the circular plots shown in Figure 3.15. A third mode of failure is caused by yielding in the top bar, in the bottom bar, and in the transverse reinforcement, all on the side where shear flows due to shear and torsion are additive, that is the left wall (Nawy, 2000). A modified form of Eqn 25a results as follows:

$$\left(\frac{V}{V_0}\right)^2 + \left(\frac{T}{T_0}\right)^2 + \sqrt{2}\left(\frac{VT}{V_0T_0}\right) = \frac{1+R}{2R} \quad (3.25b)$$

3.2 Aci Design Of Reinforced Concrete Beams Subjected To Combined Torsion Bending And Shear

3.2.1 Torsional Behavior of Structures

The torsional moment acting on a particular structural component such as a spandrel beam can be calculated using normal structural analysis procedures. Design of the particular component needs to be based on the limit state at failure. Therefore, the nonlinear behavior of a structural system after torsional cracking must be identified in one of the following two conditions: (1) no redistribution of torsional stresses to other members after cracking and (2) redistribution of torsional stresses and moments after cracking to effect deformation compatibility between intersecting members (Nawy, 2005).

Stress resultants due to torsion in statically determinate beams can be evaluated from equilibrium conditions alone. Such conditions require a design for the full-factored external torsional moment, because no redistribution of torsional stresses is possible. This state is often termed equilibrium torsion. An edge beam supporting a cantilever canopy (Nawy, 2005).

The edge beam has to be designed to resist the total external factored twisting moment due to the cantilever slab; otherwise, the structure will collapse. Failure would be caused by the beam not satisfying conditions of equilibrium of forces and moments resulting from the large external torque (Nawy, 2005).

In statically indeterminate systems, stiffness assumptions, compatibility of strains at the joints, and redistribution of stresses may affect the stress resultants, leading to a reduction in the resulting torsional shearing stresses. A reduction is permitted in the value of the factored moment used in the design of the member if part of this moment can be redistributed to the intersecting members. The ACI Code permits a maximum factored torsional moment at the critical section d from the face of the supports for reinforced concrete members as follows (Nawy, 2005) :

$$T_a = \phi 4 \sqrt{f'_c} \frac{A_{cp}^2}{P_{cp}} \quad (3.26)$$

where

A_{cp} = area enclosed by outside perimeter of concrete cross section

$$= x_0 y_0$$

P_{cp} = outside perimeter of concrete cross section A_{cp} in.

$$= 2(x_0 + y_0)$$

3.2.2 Torsional Moment Strength

The size of a cross-section is chosen on the basis of reducing unsightly cracking and preventing the crushing of the surface concrete caused by the inclined compressive stresses due to shear and torsion defined by the left-hand side of the expressions in Eqn. 27a and b. The geometrical dimensions for torsional moment strength in both reinforced and prestressed members are limited by the following expressions (Nawy, 2005).

(a) Solid sections

$$\sqrt{\left(\frac{V_u}{b_w d}\right)^2 + \left(\frac{T_u P_h}{1.7 A_{oh}^2}\right)^2} \leq \phi \left(\frac{V_c}{b_w d} + 8 \sqrt{f'_c}\right) \quad (3.27a)$$

(b) Hollow section

$$\left(\frac{V_u}{b_w d}\right) + \left(\frac{T_u P_h}{1.7 A_{oh}^2}\right) \leq \phi \left(\frac{V_c}{b_w d} + 8 \sqrt{f'_c}\right) \quad (3.27b)$$

CHAPTER 4

NEURAL NETWORKS

4.1 Neural Networks Systems

4.1.1 Neural Networks

NN is a computational tool, which attempts to simulate the architecture and internal operational features of the human brain and nervous system. NN architectures are formed by three or more layers, which includes an input layer, an output layer and a number of hidden layers in which neurons are connected to each other with modifiable weighted interconnections Pala et al.(2008). Each neuron has an associated transfer function, which describes how the weighted sum of its inputs is converted to the results into an output value. Each hidden or output neuron receives a number of weighted input signals from each of the units of the preceding layer and generates only one output value. This NN architecture is commonly referred to as a fully interconnected feedforward multi-layer perceptron. In addition, there is also a bias, which is only connected to neurons in the hidden and output layers with modifiable weighted connections. The number of neurons in each layer may vary depending on the problem (Moiler,1993).

Artificial Intelligence (AI) comprises methods, tools, and systems for solving problems that normally require the intelligence of humans. The term intelligence is always defined as the ability to learn effectively, to react adaptively, to make proper decisions, to communicate in language or images in a sophisticated way, and to understand. The main objectives of AI are to develop methods and systems for solving problems, usually solved by the intellectual activity of humans, for example, image recognition, language and speech processing, planning, and prediction, thus enhancing computer information systems; and to develop models which simulate living organisms and the human brain in particular, thus improving our understanding of how the human brain works (Kasabov,1996).

The main AI directions of development are to develop methods and systems for solving AI problems without following the way humans do so, but providing similar results, for example, expert systems; and to develop methods and systems for solving AI problems by modeling the human way of thinking or the way the brain works physically, for example, artificial neural networks (Kasabov,1996).

Artificial Neural Networks (ANN) can be defined as computer models that mimic the biological nervous system in general. There are many definitions of NNs in literature which can be summarized as follows:

A Neural Network is a ‘machine’ that is designed to model the way in which the brain performs a particular task or function of interest, the network is usually implemented using electronic components or simulated in software on a digital computer (Hecht-Neilsen,1990).

(Haykin,1994) defines a neural network as a massively parallel distributed processor that has a natural propensity for storing experiential knowledge and making it available for use. It resembles the brain in two respects:

- Knowledge is acquired by the network through a learning process.
- Interneuron connection strengths known as synaptic weights are used to store the knowledge.

On the other hand according to (Nigrin,1993); a neural network is a circuit composed of a very large number of simple processing elements that are neural based. Each element operates only on local information. Furthermore each element operates asynchronously; thus there is no overall system clock. Another widely accepted definition of NNs is given by to (Zurada,1992) as follows: Artificial neural systems, or neural networks, are physical cellular systems which can acquire, store, and utilize experiential knowledge.

4.1.2 History of Neural Networks

The first step toward artificial neural networks came in 1943 when Warren McCulloch, a neurophysiologist, and a young mathematician, Walter Pitts, wrote a paper on how neurons might work. They modeled a simple neural network with electrical circuits. In 1949, Donald Hebb proposed 'Hebb rule' which states that nets can learn from their experience in a training environment. 'Hebb rule' has always played a striking role in the field of ANN studies (Hebb,1949). Throughout 1950s scientists implemented models called perceptrons based on the work of McCulloch and Pitts. In 1957, Rosenblatt invented the *Perceptron* which has been a milestone in ANN studies. Widrow and Hoff developed the models called ADALINE and MADALINE in 1959 which was the first neural network to be applied to a real world problem. In 1968, Marvin Minsky published some intrinsic limitations of neural Networks which slowed down the implementations of ANN drastically Minsky and Pappert, (1969). The studies in the field ANN almost stopped for more than a decade until Hopfield invented The Hopfield network in 1982 whose dynamics were guaranteed to converge. After this novel invention, ANN studies have raised again. Backpropagation was invented in 1986 by Rumelhart, Hinton and Williams which opened a new era in ANN applications Rumelhart et al.(1986).

4.1.3 Elements of Neural Networks

The basic element of a neural network is the artificial neuron which is actually the mathematical models of biological neuron model shown in Figure 4.1. A biological neuron is made up of four main parts: dendrites, synapses, axon and the cell body. The dendrites receive signals from other neurons. The axon of a single neuron serves to form synaptic connections with other neurons. The cell body of a neuron sums the incoming signals from dendrites (Çevik,2006).

If input signals are sufficient to stimulate the neuron to its threshold level, the neuron sends an impulse to its axon. On the other hand, if the inputs do not reach the required level, no impulse will occur. The analogy between a biological neuron model and an artificial neuron model is shown in Figure 4.1 and Figure 4.2. (Çevik,2006).

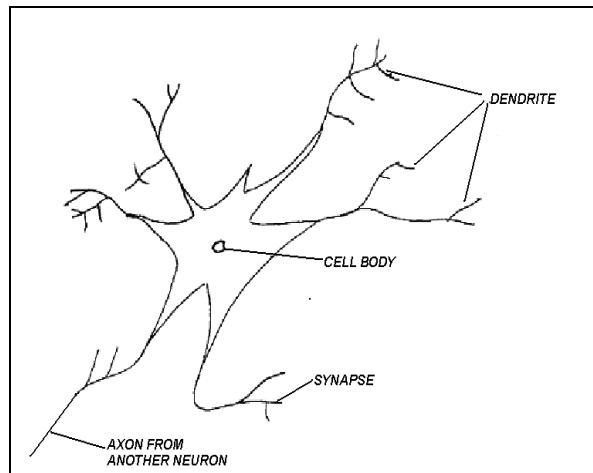


Fig4.1 A biological neuron (Wasserman,1989).

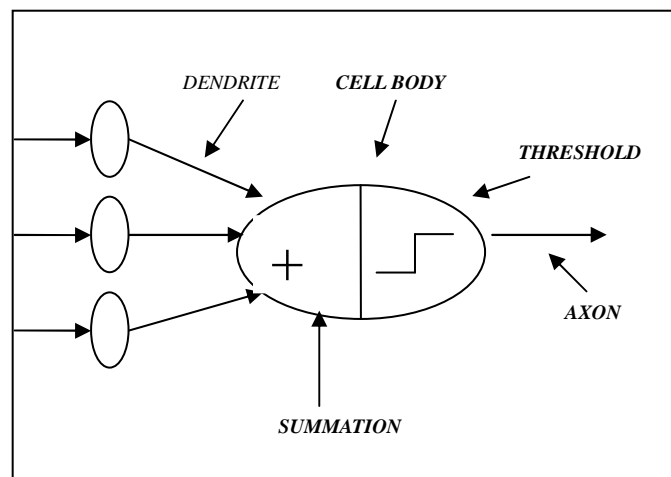


Fig 4.2 Artificial neuron model (Çevik,2006).

The artificial neuron consists of three main components namely as weights, bias, and an activation function Fig 4.3. Each neuron receives inputs x_1, x_2, \dots, x_n , attached with a weight w_i which shows the connection strength for that input for each connection. Each input is then multiplied by the corresponding weight of the neuron connection. A bias b_i can be defined as a type of connection weight with a constant nonzero value added to the summation of inputs Fig 4.3 and corresponding weights u , given in Eqn4.1 (Çevik,2006).

$$u_i = \sum_{j=1}^H w_{ij} x_j + b_i \quad (4.1)$$

The summation u_i is transformed using a scalar-to-scalar function called an "activation or transfer function", $F(u_i)$ yielding a value called the unit's "activation", given in Eqn4.2.

$$Y_i = f(u_i) \quad (4.2)$$

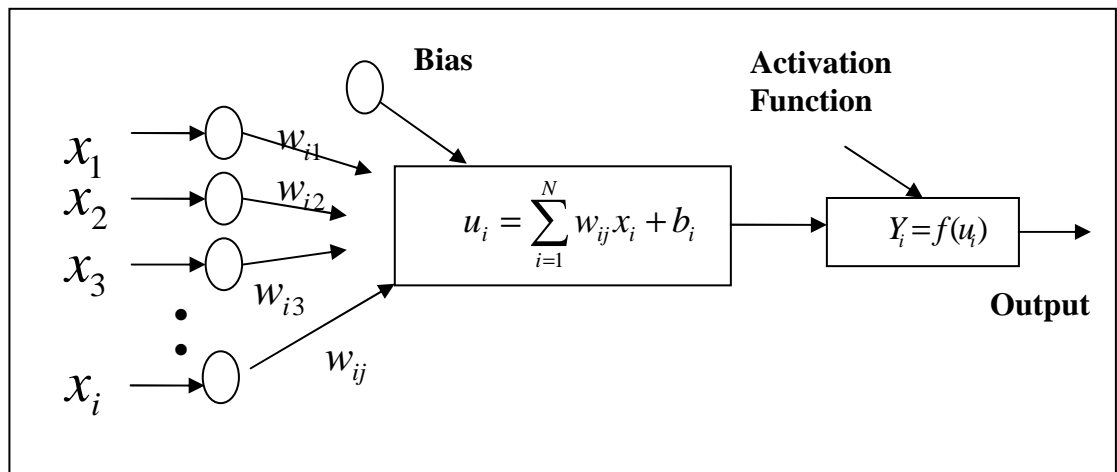


Fig4.3 Basic elements of an artificial neuron (Çevik,2006).

Activation functions serve to introduce nonlinearity into neural networks which makes NNs so powerful. The activation function is also referred to as a squashing function. There are a number of different types of activation function and some common examples are provided below (Çevik,2006):

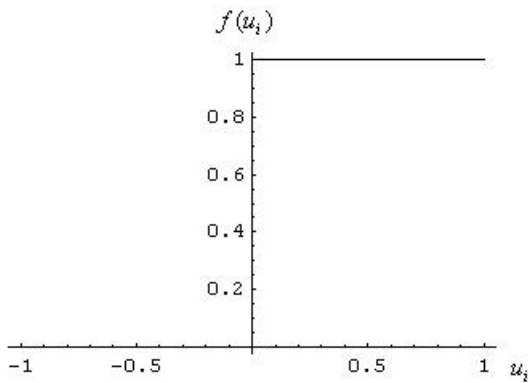


Fig4.4 Threshold activation function.

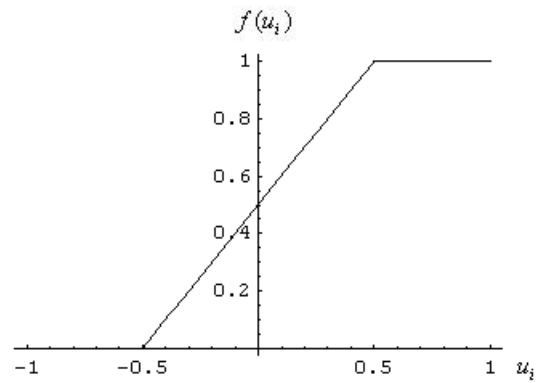


Fig4.5 Piecewise-linear function

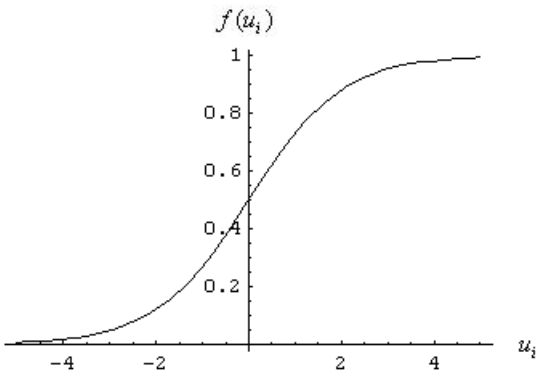


Fig4.6 Sigmoid (logistic) function.

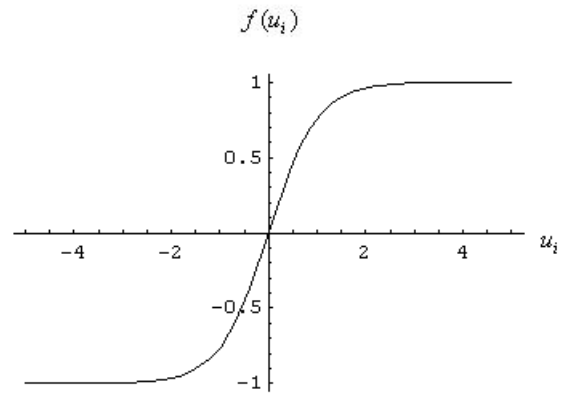


Fig4.7 Hyperbolic tangent function.

Guzelbey et al.(2006) have proposed an alternative approach for the prediction of web crippling strength of cold-formed steel sheeting using NNs. They have presented the proposed NN model in a closed form solution with a very high correlation ($R = 0.995$) compared with experimental results from the literature. The well trained NN model has also been used to conduct parametric studies.

4.1.4 Classification of Neural Networks

Neural Network models can be classified in a number of ways. Using the network architecture as basis, there are three major types of neural networks:

Recurrent networks - the units are usually laid out in a two-dimensional array and are regularly connected. Typically, each unit sends its output to every other unit of the network and receives input from these same units. Recurrent networks are also called *feedback networks*. Such networks are "clamped" to some initial configuration by setting the activation values of each of the units. The network then goes through a stabilization process where the network units change their activation values and slowly evolve and converge toward a final configuration of "low energy". The final configuration of the network after stabilization constitutes the output or response of the network. This is the architecture of the Hopfield Model (www.comp.nus.edu.sg)

Feed forward networks – these networks distinguish between three types of units: input units, hidden units, and output units. The activity of this type of network propagates forward from one layer to the next, starting from the input layer up to the output layer. Sometimes called multilayered networks, feed forward networks are very popular because this is the inherent architecture of the Backpropagation Model. (Çevik,2006).

Competitive networks– these networks are characterized by lateral inhibitory connections between units within a layer such that the competition process between units causes the initially most active unit to be the only unit to remain active, while all the other units in the cluster will slowly be deactivated. This is referred to as a "winner-takes-all" mechanism. Self-Organizing Maps, Adaptive Resonance Theory, and Rumelhart & Zipser's Competitive Learning Model are the best examples for these types of networks. (www.comp.nus.edu.sg)

The network architecture can be further subdivided into whether the network structure is fixed or not. There are two broad categories (Çevik,2006) :

- *Static architecture* – most of the seminal work on neural networks were based on static network structures, whose interconnectivity patterns are fixed *a priori*, although the connection weights themselves are still subject to training. Perceptrons, multi-layered perceptrons, self-organizing maps, and Hopfield networks all have static architecture.

- *Dynamic architecture* – some neural networks do not constrain the network to a fixed structure but instead allow nodes and connections to be added and removed as needed during the learning process as adaptivity. Some examples are Grossberg’s Adaptive Resonance Theory and Fritzke’s “Neural Gas”. Some adding-pruning approaches to Multi-Layered Perceptron networks have also been widely studied.

Yet another basis for classifying neural network models is according to the mode of learning adapted. In this case, there are two major categories.(www.comp.nus.edu.sg)

- *Supervised learning* – these are generally the learn-by-example methods where user-supplied information are provided with each training pattern. These guide the neural network in adjusting its parameters. The perceptrons and backpropagation networks are classic examples of supervised learning models.
- *Unsupervised learning* – some neural network models do not need category information to accompany each training pattern, although such information would still be required in the interpretation and labeling of the resultant networks. Classical examples of these are Kohonen’s self-organizing maps and Grossberg’s Adaptive Resonance Theory.

It also makes sense to classify neural network models on the basis of their over-all task(Çevik,2006):

- *Pattern association* – the neural network serves as an associative memory by retrieving an associated output pattern given some input pattern. The association can be *auto-associative* or *hetero-associative*, depending on whether or not the input and output patterns belong to the same set of patterns.

- *Classification* – the network seeks to divide the set of training patterns into a pre-specified number of categories. Binary-valued output values are generally used for classification, although continuous-valued outputs (coupled with a labeling procedure) can do classification just as well.
- *Function approximation* – the network is supposed to compute some mathematical function. The network's output represents the approximated value of the function given the input pattern as parameters. In certain areas, *regression* may be the more natural term.

There are other bases for classifying neural network models, but these are less fundamental than those mentioned earlier. Some of these include the type of input patterns that can be admitted (binary, discrete valued, real values), or the type of output values that are produced. (www.comp.nus.edu.sg)

4.1.5 Back propagation Algorithm

Back propagation algorithm is one of the most widely used supervised training methods for training multilayer neural networks due to its simplicity and applicability. It is based on the generalized delta rule and was popularized by Rumelhart and coworkers Rumelhart et al.(1986). As it is a supervised learning algorithm, there is a pair of inputs and corresponding output. The algorithm is simply based on a weight correction procedure shown schematically in Fig4.8 .It consists of two passes: a forward pass and a backward pass. In the forward pass, first, the weights of the network are randomly initialized and an output set is obtained for a given input set where weights are kept as fixed. The error between the output of the network and the target value is propagated backward during the backward pass and used to update the weights of the previous layers as shown in Fig4.9 (Zupan,1993).

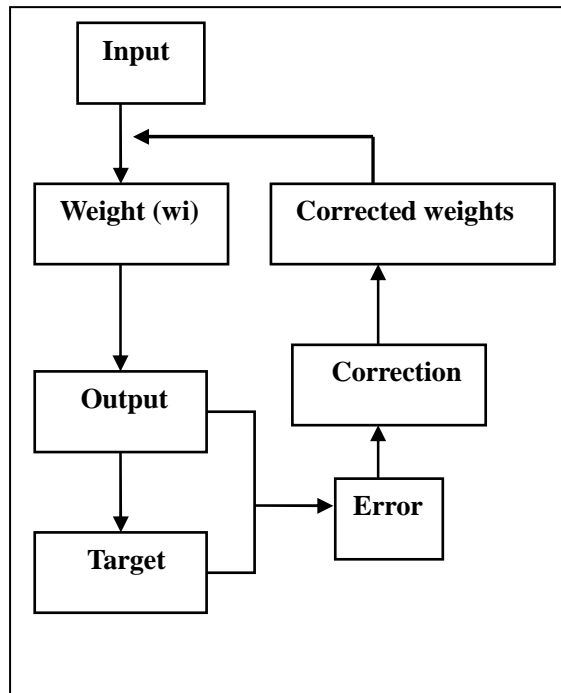


Fig4.8 Schematic presentation of weight correction in BPNN(Çevik,2006).

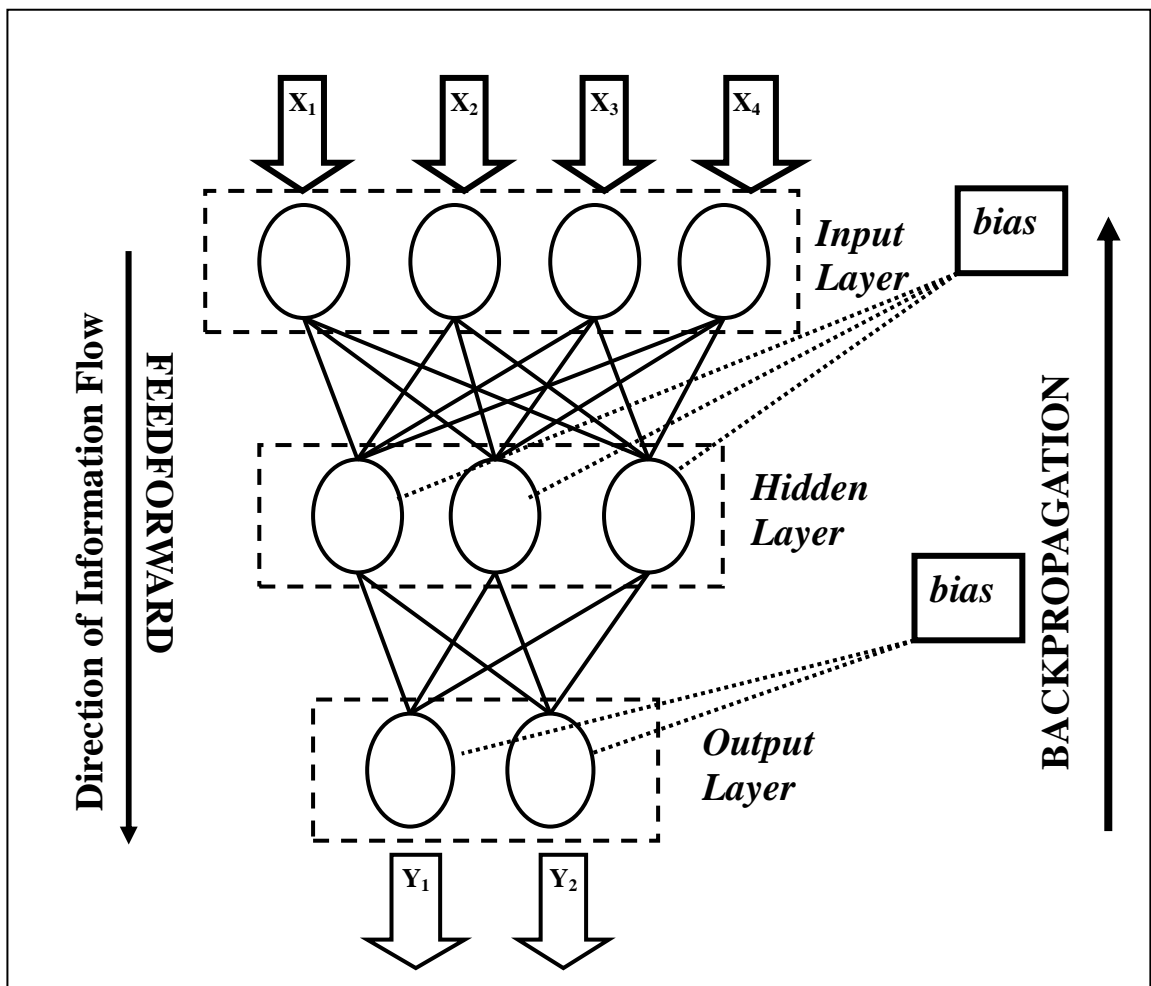


Fig4.9 Back propagation algorithm(Çevik,2006).

The main goal of BPNN is mapping of input, i.e. vector \mathbf{x} into output, i.e. vector \mathbf{y} .: This can be written in short:

$$X_i \xrightarrow{BPNN} Y_i \quad (4.3)$$

For the output layer the error δ_j^{last} can be given as the difference between the target value Y_i and the network output out_j^{last} :

$$\delta_j^{last} = (Y_i - out_j^{last})out_j^{last} (1 - out_j^{last}) \quad (4.4)$$

The weight correction is given as

$$\Delta w_{ji}^l = w_{ji}^{l(new)} - w_{ji}^{l(old)} \quad (4.5)$$

Combining Eqn4.4 and 4.5 the weight correction in a hidden layer can be generalized as follows:

$$\Delta w_{ji}^l = \eta \left(\sum_{k=1}^r \delta_k^{l+1} w_{kj}^{l+1} \right) out_j^l (1 - out_j^l) out_i^{l-1} + \mu \Delta w_{ji}^{l(previous)} \quad (4.6)$$

where η is the learning rate and μ is the momentum constant .

Eqn4.5 can be also be expressed in condensed form as:

$$\Delta w_{ji}^l = \eta \delta_j^l out_i^{l-1} + \mu \Delta w_{ji}^{l(previous)} \quad (4.7)$$

4.1.6 Matlab NN Toolbox

In this thesis, Matlab NN toolbox is used for NN modeling. Matlab NN toolbox is preferred due to its flexibility. As a result, an optimal NN selection algorithm program has been developed which is almost impossible for other NN software available in market.

The toolbox consists of a set of functions and structures that handle neural networks, so the user does not need to write code for all activation functions, training algorithms. The toolbox is based on the network object. This object contains information about everything that concern the neural network, e.g. the number and structure of its layers, the connectivity between the layers, etc. Matlab provides high-level network creation functions, like `newlin` (create a linear layer), `newp` (create a perceptron) or `newff` (create a feed-forward backpropagation network) to allow an easy construction (Çevik,2006).

A graphical user interface has been added to the toolbox. This interface allows you to:

- Create networks
- Enter data into the GUI
- Initialize, train, and simulate networks
- Export the training results from the GUI to the command line workspace
- Import data from the command line workspace to the GUI

The User can handle almost all main parameters related with NN model and obtain them very easily. Architecture parameters and the subobject structures given by the Toolbox are as follows:

inputs: {1x1 cell} of inputs

layers: {1x1 cell} of layers

outputs: {1x1 cell} containing 1 output

targets: {1x1 cell} containing 1 target

biases: {1x1 cell} containing 1 bias

inputWeights: {1x1 cell} containing 1 input weight

layerWeights: {1x1 cell} containing no layer weights

In this thesis, by the aid of these NN parameters, closed form solutions of the proposed NN models are also derived and presented. This will open the black box as NNs are often referred to as. The analytical form of the NN models will enable them to be used for further practical applications(Çevik,2006).

4.1.7 Optimal NN Model Selection

The performance of a NN model mainly depends on the network architecture and parameter settings. One of the most difficult tasks in NN studies is to find this optimal Network architecture which is based on determination of numbers of optimal layers and neurons in the hidden layers by trial and error approach. The assignment of initial weights and other related parameters may also influence the performance of the NN in a great extent. However there is no well defined rule or procedure to have optimal network architecture and parameter settings where trial and error method still remains valid. This process is very time consuming Çevik and Güzelbey,(2008).

Various Backpropagation Training Algorithms are used in this thesis given in Table4.1. Matlab NN toolbox randomly assigns the initial weights for each run each time which considerably changes the performance of the trained NN even all parameters and NN architecture are kept constant. This leads to extra difficulties in the selection of optimal Network architecture and parameter settings. To overcome this difficulty, a program has been developed in Matlab which handles the trial and error process automatically (Çevik,2006).

The program tries various number of layers and neurons in the hidden layers both for first and second hidden layers for a constant epoch for several times and selects the best NN architecture with the minimum MAPE (Mean Absolute % Error) or RMSE (Root Mean Squared Error) of the testing set, as the training of the testing set is more critical. For instance, NN architecture with 1 hidden layer with 7 nodes is tested 10 times and the best NN is stored where in the second cycle the number of hidden nodes is increased up to 8 and the process is repeated. The best NN for cycle 8 is compared with cycle 7 and the best one is stored as best NN. Tapkın et al.(2010). This process is repeated N times where N denotes the number of hidden nodes for the first hidden layer. This whole process is repeated for changing number of nodes in the second hidden layer. Moreover, this selection process is performed for different back propagation training algorithms such as trainlm, trainscg and trainbfg given in Table4.1. The program begins with simplest NN architecture i.e. NN with 1 hidden node for the first and second hidden layers and ends up with optimal NN architecture as shown in Figure4.10.The whole process is shown in Figure4.11(Çevik,2006).

Table4.1. Back propagation training algorithms used in NN training Çevik et al.(2008).

MATLAB Function name	Algorithm
trainbfg	BFGS quasi-Newton back propagation
traincgf	Fletcher-Powell conjugate gradient back propagation
traincgp	Polak-Ribiere conjugate gradient back propagation
traingd	Gradient descent back propagation
traingda	Gradient descent with adaptive lr back propagation
traingdx	Gradient descent w/momentum & adaptive linear back propagation
trainlm	Levenberg-Marquardt back propagation
trainoss	One step secant back propagation
trainrpf	Resilient back propagation (Rprop)
trainscg	Scaled conjugate gradient back propagation

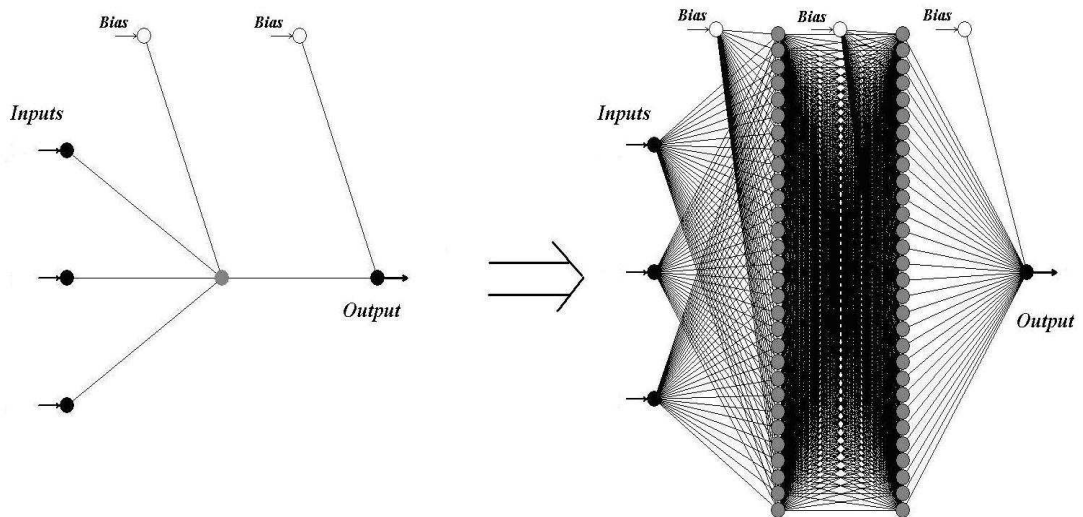


Fig4.10 Optimal NN selection process Çevik and Güzelbey,(2008).

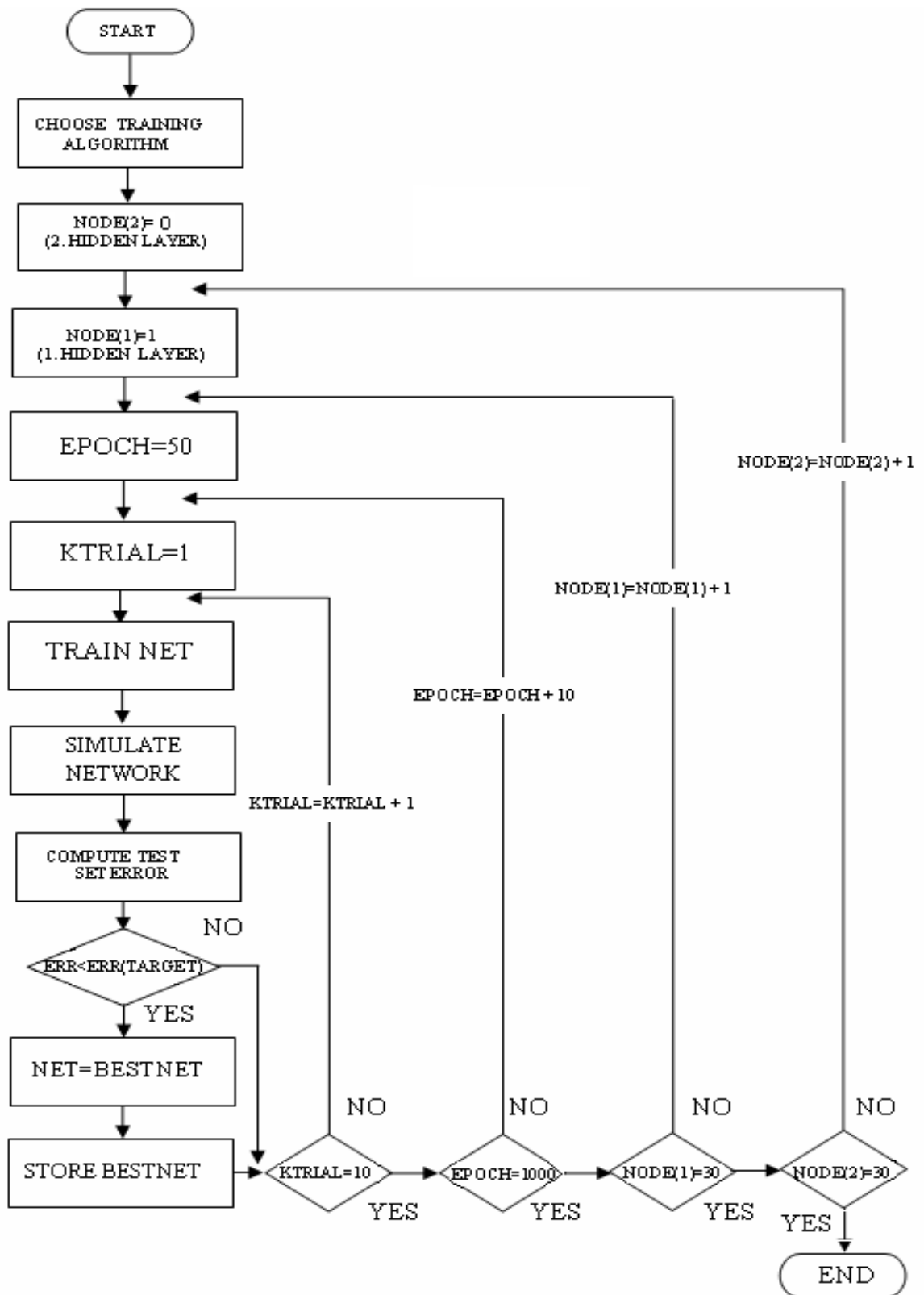


Fig4.11 Flowchart of optimal NN selection. Çabalar and Çevik,(2009).

CHAPTER 5

NUMERICAL APPLICATION

5.1 Selection of Database (Description of data)

The experimental data considered here was obtained from different papers: Rasmussen and Baker (1995), Koutchoukali and Belarbi (2001), Fang and Shiau (2004), Hsu(1968), Tang(2006), Zang(2002) . The test specimens were of solid rectangular beams which were subjected in pure tension and none of them were deep beams. The compressive strength of concrete ranged from 25.58 MPa to 109.8 MPa, stirrup percentage ranged from 0.40 % to 2.56 %, the yielding stress of longitudinal reinforcement ranged from 314 MPa to 560 MPa, the yielding stress of stirrups ranged from 320 MPa to 672 MPa. The complete list of the data is given in the Appendix section. As it is seen from the Table appendix, a total of 76 tests satisfying the variables mentioned above. Beams are identified using the notations in the first row, with the first letter of researchers' name. The same series of test was used before by several authors. Tang (2006), developed a radial basis function neural networks to predict the ultimate torsional strength of RC beams, Zhang (2002), and Hossain et al. (2006) improved analytical methods for predicting the nonlinear response of RC beams by using the test.

5.2 Numerical Application of NN

In this study, MATLAB neural network toolbox was used to estimate the torsional strength of RC beams. The feed-forward multilayer network with error-back propagation model consists of twelve input nodes and one output node. They tested numerous RC beams under pure torsion to measure cracking (T_{cr}) and ultimate torque (T_u).

A total of 76 RC beams having different geometric parameters such as dimension of the cross section (x , y), dimension of the closed stirrup (x_1 , y_1), concrete compressive strength (f_c), spacing of stirrups (s), cross-sectional area of one leg of closed stirrup (A_t), yield strength of closed stirrup (f_{yv}), total area of longitudinal torsional reinforcement (A_t), yield strength of longitudinal torsional reinforcement (f_{yl}), steel ratio of stirrups (ρ_t) and steel ratio of longitudinal reinforcement (ρ_l). The range of datasets is listed in Table 5.1. (M.H Arslan ,2010)

Table 5.1 Data Range

	Minimum	Maximum	Increment
x (mm)	160	350	Variable
y (mm)	275	508	Variable
x_1 (mm)	130	300	Variable
y_1 (mm)	216	469	Variable
f_c (MPa)	26	110	Variable
s (mm)	50	215	Variable
A_t (mm ²)	71	127	Variable
f_{yv} (MPa)	319	672	Variable
A_l (mm ²)	381	3438	Variable
f_{yl} (MPa)	310	638	Variable
ρ_t (%)	0.22	2.56	Variable
ρ_l (%)	0.30	3.51	Variable

From the set of 76 total data, %80 of data sets were selected for training set for neural network training and the others are for testing.

Among 12 input nodes (as x , y , x_1 , y_1 , f_c , s , A_t , f_{yv} , A_t , f_{yl} , ρ_t and ρ_l), 2 different NN models were constructed. The first model consists of 5 input parameters namely as A_c , A_t f_{yt}/s , $ALfyL$, $f'c$, P_c where as the other consists of 7 input parameters namely as r_t , r_l , A_c , P_c , $f'c$, $ALfyL$, A_t f_{yt}/s .

The optimal NN architecture in this part was found to be 5-3-1 (5 inputs- 3 hidden neurons- 1 output) NN architecture with logistic sigmoid transfer function (logsig) for the first NN model. The optimal NN architecture in this part was found to be 7-3-1 (7 inputs- 3 hidden neurons- 1 output) NN architecture with logistic sigmoid transfer function (logsig) for the second NN model.

The training algorithm was quasi-Newton back propagation (BFGS). The statistical parameters of the NN models are given in Tables 5.2 and 5.3.

COV (Coeff. Of Variation) is derived from standart deviation divided by means of data (data is experimental torsional data divided by NN model torsional data) and R^2 (Coeff. Of Correlation) is the graphic of experimantel torsional date and NN model torsional data. According to COV and R^2 , it is seen that the NN models gives more accurate results.

Table 5.2 Statistical parameters of testing and training sets and overall results of NN model 1

	Mean	Std. Dev.	COV	R2
Testing Set	1.017	0.307	0.302	0.85
Training Set	1.033	0.229	0.222	0.95
Total Set	1.029	0.244	0.237	0.94

Table 5.3 Statistical parameters of testing and training sets and overall results of NN model 2

	Mean	Std. Dev.	COV	R2
Testing Set	1.009	0.129	0.128	0.98
Training Set	1.019	0.137	0.134	0.98
Total Set	1.017	0.134	0.132	0.98

The performance of the proposed NN models vs. experimental results are given in Figure 5.1 and 5.2. The accuracy of the formulation is observed to be quite good, it should be noted that the proposed NF model presented is valid only for the ranges of variables of the experimental database.

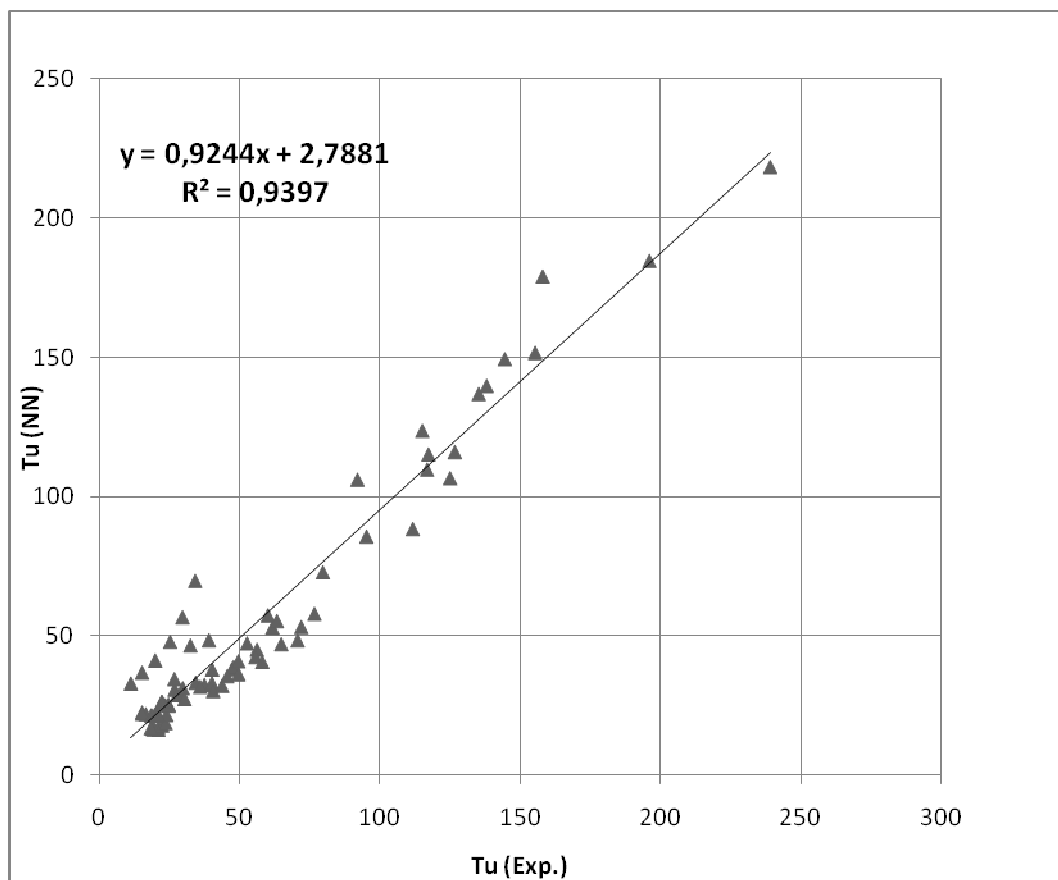


Fig 5.1 Experimental results graphic of NN model 1

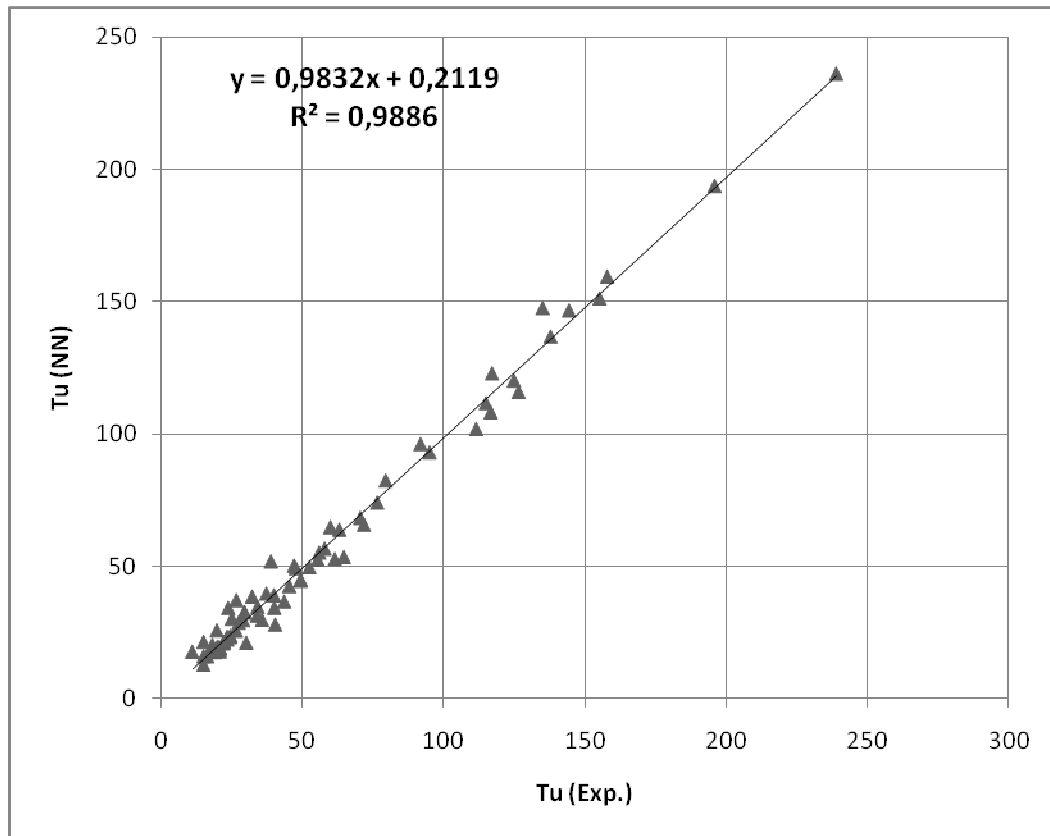


Fig5.2 Experimental results graphic of NN model 2

5.3 Explicit Formulation of NN Model

NN applications are treated as black-box applications in general. However this study opens this black box and introduces the NN application in a closed form solution.

NN model 1 and 2 can be computed as follows:

NN model 1;

$$IN_0 = Ac * 6.10687e-06 - 0.168702$$

$$IN_1 = Pc * 0.000963855 - 0.738554$$

$$IN_2 = f'c * 0.00949893 - 0.142983$$

$$IN_3 = "AL\ fyL" * 4.45621e-07 + 0.0420553$$

$$IN_4 = "At\ fyt/s" * 0.000888057 - 0.000134556$$

$$HL_0 = \text{sigmoid}(-1.46315 * IN_0 - 0.180801 * IN_1 - 2.26827 * IN_2 - 1.28312 * IN_3 - 0.684621 * IN_4 + 4.75584)$$

$$HL_1 = \text{sigmoid}(-2.67591 * IN_0 - 2.50177 * IN_1 + 1.37961 * IN_2 + 0.887238 * IN_3 - 0.182111 * IN_4 - 0.808109)$$

$$HL_2 = \text{sigmoid}(-1.4407 * IN_0 + 0.146792 * IN_1 - 0.464883 * IN_2 - 1.85803 * IN_3 - 1.81356 * IN_4 + 2.37321)$$

$$OUT = (\text{sigmoid}(-3.59922 * HL_0 - 2.29963 * HL_1 - 2.32142 * HL_2 + 3.73206) - 0.0602986) / 0.00351339$$

Where $\text{sigmoid}(x) = 1 / (1 + \exp(x))$

NN model 2;

$$IN_0 = rt * 0.34188 + 0.0247863$$

$$IN_1 = rl * 0.249221 + 0.0252336$$

$$IN_2 = Ac * 6.10687e-06 - 0.168702$$

$$IN_3 = Pc * 0.000963855 - 0.738554$$

$$IN_4 = f'c * 0.00949893 - 0.142983$$

$$IN_5 = "AL fyL" * 4.45621e-07 + 0.0420553$$

$$IN_6 = "At fyt/s" * 0.000888057 - 0.000134556$$

$$HL_0 = \text{sigmoid}(-0.0141111 * IN_0 - 1.44714 * IN_1 - 2.55339 * IN_2 - 0.788241 * IN_3 - 4.18833 * IN_4 - 0.60156 * IN_5 + 3.44565 * IN_6 - 0.784084)$$

$$HL_1 = \text{sigmoid}(3.7208 * IN_0 - 1.82187 * IN_1 + 4.02579 * IN_2 - 3.01756 * IN_3 - 1.06721 * IN_4 + 2.82985 * IN_5 - 1.48013 * IN_6 - 0.185655)$$

$$HL_2 = \text{sigmoid}(1.32497 * IN_0 + 0.845099 * IN_1 - 2.21704 * IN_2 + 0.993666 * IN_3 - 3.79075 * IN_4 - 1.39997 * IN_5 - 2.25887 * IN_6 + 5.92047)$$

$$OUT = (\text{sigmoid}(-4.43372 * HL_0 + 5.07986 * HL_1 - 5.90746 * HL_2 + 1.12334) - 0.0602986) / 0.00351339$$

Where $\text{sigmoid}(x) = 1/(1+\exp(-x))$

In order to investigate the accuracy of standards for torsional strength, the test results given in Table 5.4 were compared with the approaches of mentioned building codes. The predicting capability of codes related to torsional strength of the beams for mentioned tested 76 specimens are presented in Table 5.4.

Table 5.4 Predicting capability of building code approaches

Building Standards	Expression for torsional strength	R ² (%)
ACI-318-2005	$T_n = \frac{2A_o A_t f_{yv}}{s} \cot \theta$	85.93
BS8110	$T_n = \frac{0.8x_1 y_1 (0.87f_{ys}) A_{sv}}{s}$	81.76
TBC-500-2000	$T_n = \frac{2A_e A_e f_{yv}}{2(x_1 + y_1)}$	71.07
AS3600	$T_n = \frac{2A_o A_t f_{yv}}{s} \cot \theta$	85.93
Eurocode-2-01	$T_n = f_{ys} (A_{sw} / s) 2A_k \cot \theta$	73.44
Eurocode-2-02	$T_n = f_y (A_s / u_k) 2A_k \tan \theta$	85.93
Eurocode-2-03	$T_n = 1.2(1 - f_{ck} / 250) f_{ck} A_k t_{ef} \sin \theta \cos \theta$	61.88
CSA	$T_n = \frac{2A_o A_t f_{yv}}{s} \cot \theta$	85.93
NN model1		94
NN model2		98

5.4 Main Effects of Variables

The “Main Effect Plot” is an important graphical tool to visualize the independent impact of each variable on output. This graphical tool enables a better and simple picture of the overall importance of variable effects on the output and will provide a general snapshot.

Moreover, parametric studies have also been presented as 2D and 3D surface interaction diagrams shown in Figures 5.5 - 5.8. The main effects plot will also help further researchers willing to perform experimental studies in the phase of design of experiments.

The main effects plot will also help further researchers willing to perform experimental studies in the phase of design of experiments. 2D and 3D surface interaction diagrams will be very helpful for the people who want to use proposed NN models because they show combination of the interaction of two variables.

When there is a need of NN models in one application, different combination of models with different model parameters can be selected which satisfy the requirements of the application. Using the 2D and 3D surface interaction diagrams, it is possible to select the most reliable NN model out of the possible NN models since the effect of each parameter for a prescribed another parameter can be determined.

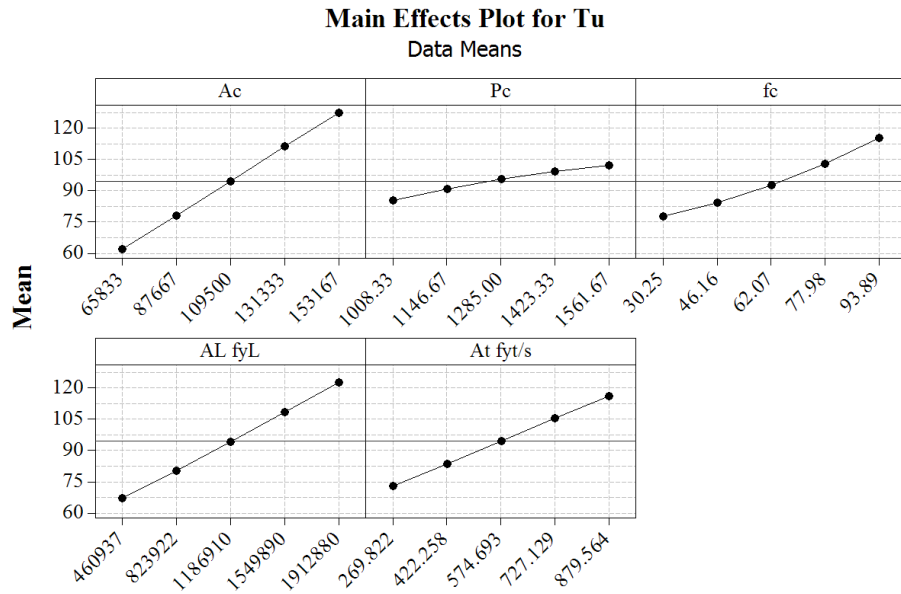


Fig5.3 Main Effects Plot for NN model 1

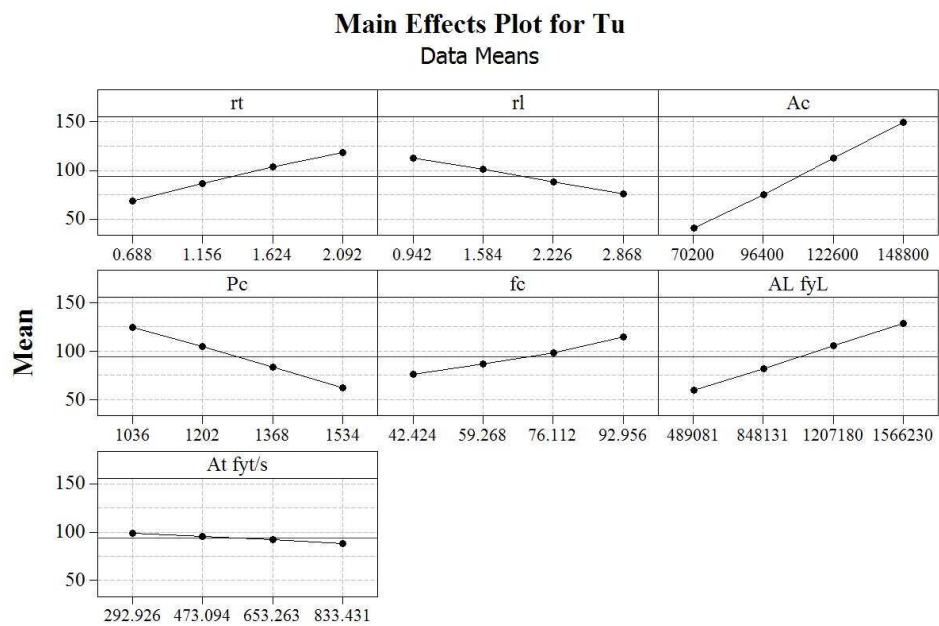


Fig5.4 Main Effects Plot for NN model 2

Interaction Plot for Tu

Data Means

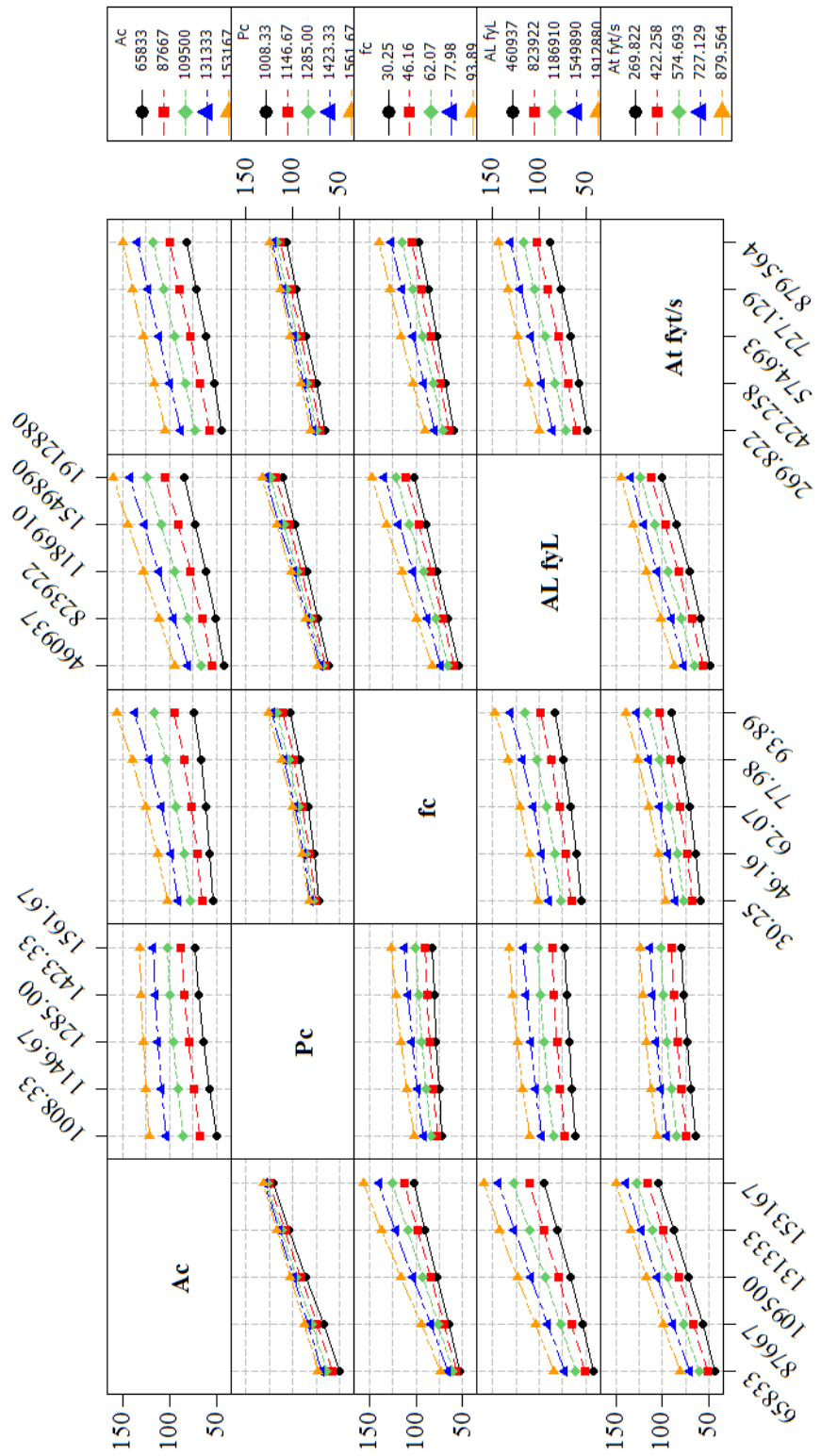


Fig5.5 2D Parametric Study for NN model 1

Interaction Plot for Tu Data Means

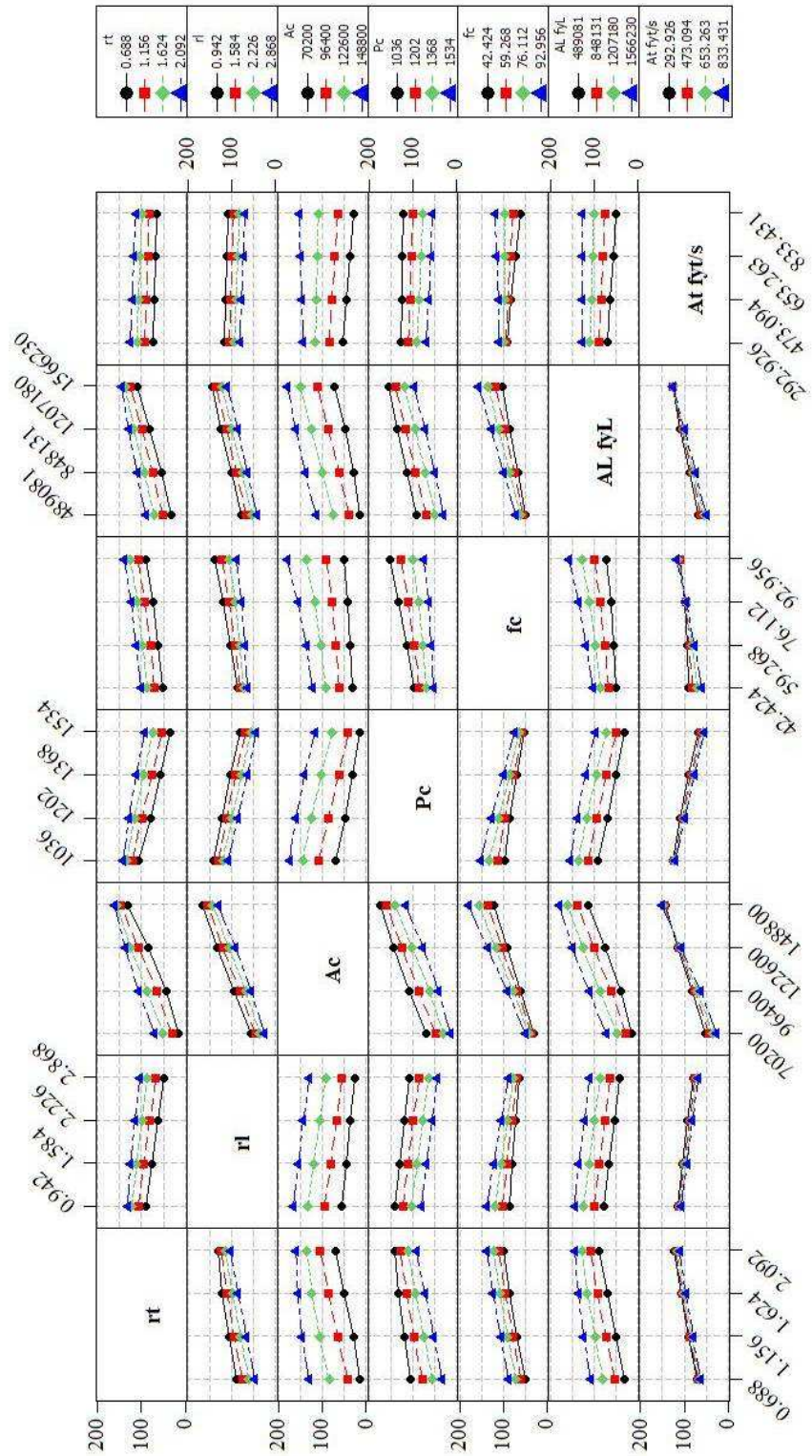
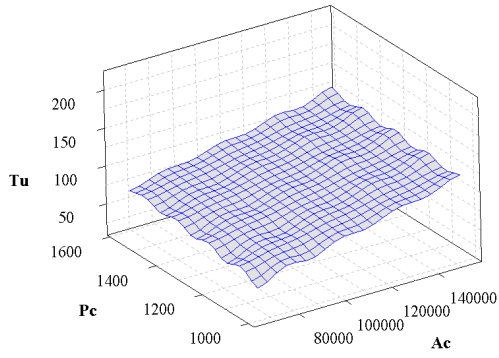


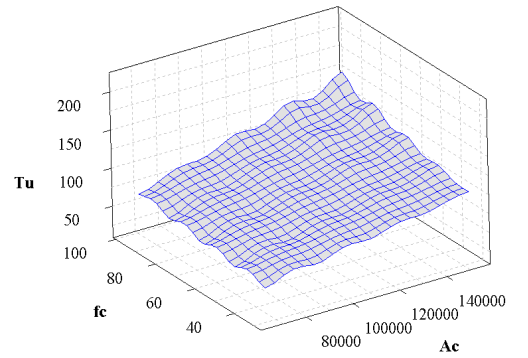
Fig5.6 2D Parametric Study for NN model 2

Surface Plot of Tu vs Pc, Ac



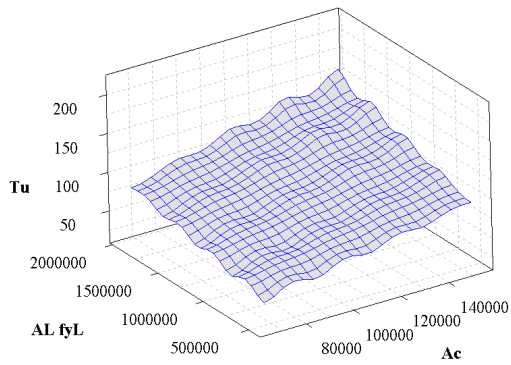
(a)

Surface Plot of Tu vs fc, Ac



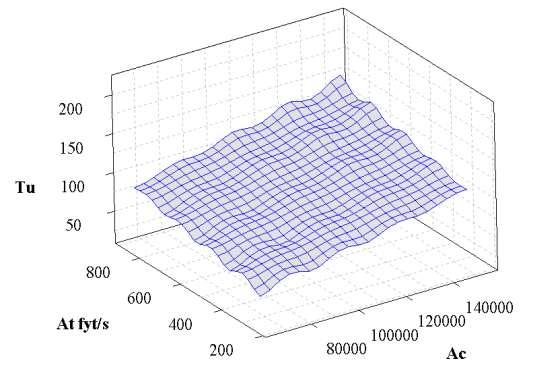
(b)

Surface Plot of Tu vs AL fyL, Ac



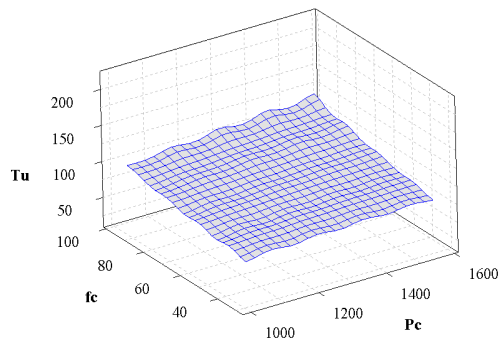
(c)

Surface Plot of Tu vs At fyL/s, Ac



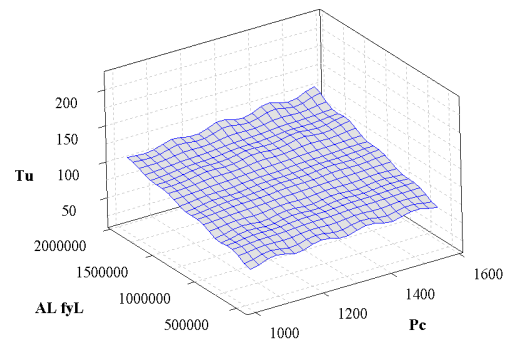
(d)

Surface Plot of Tu vs fc, Pc



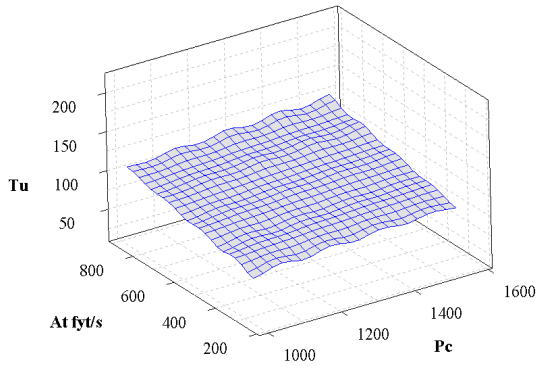
(e)

Surface Plot of Tu vs AL fyL, Pc



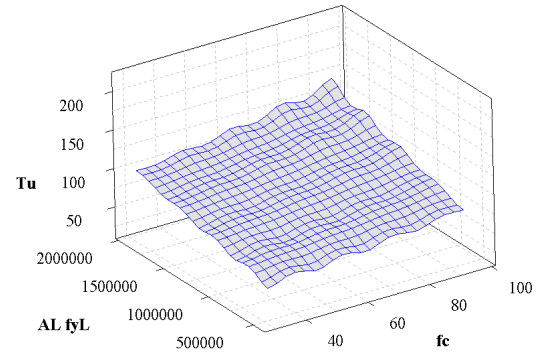
(f)

Surface Plot of Tu vs At fyt/s, Pc



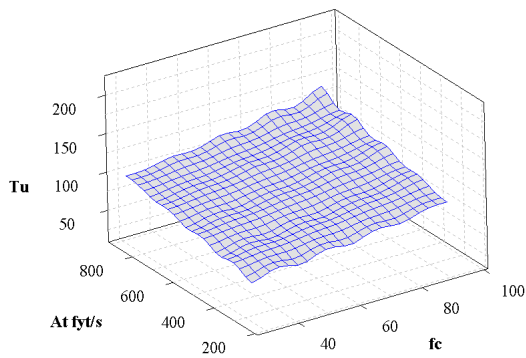
(g)

Surface Plot of Tu vs AL fyL, fc



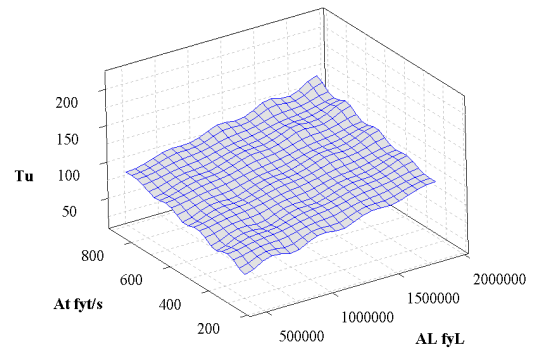
(h)

Surface Plot of Tu vs At fyt/s, fc



(i)

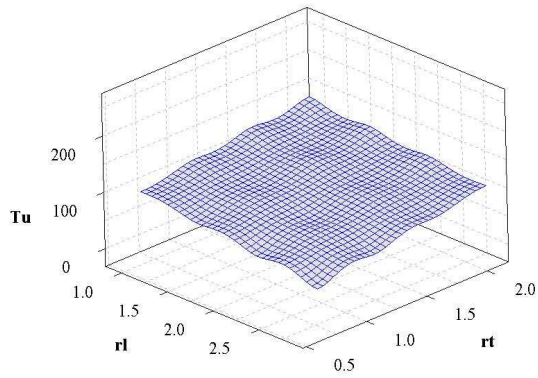
Surface Plot of Tu vs At fyt/s, AL fyL



(j)

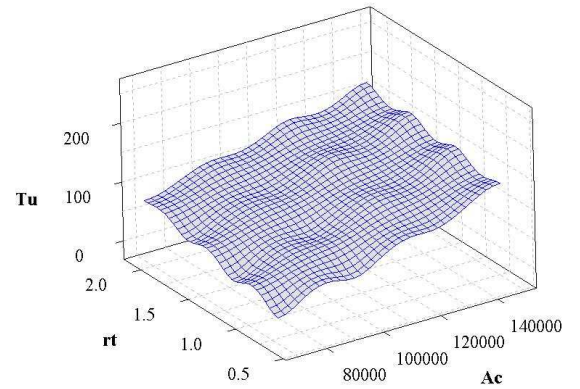
Fig5.7 3D Parametric Study for NN model 1

Surface Plot of Tu vs rt, rl



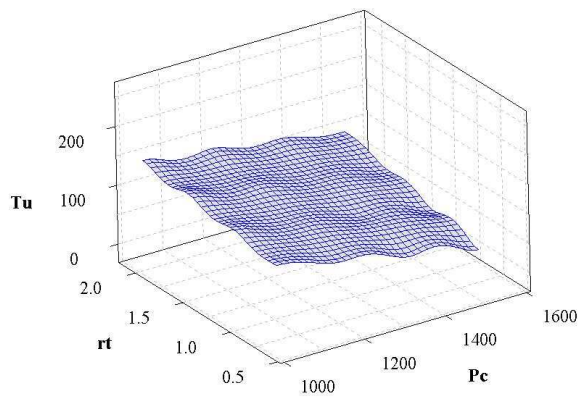
(a)

Surface Plot of Tu vs rt, Ac



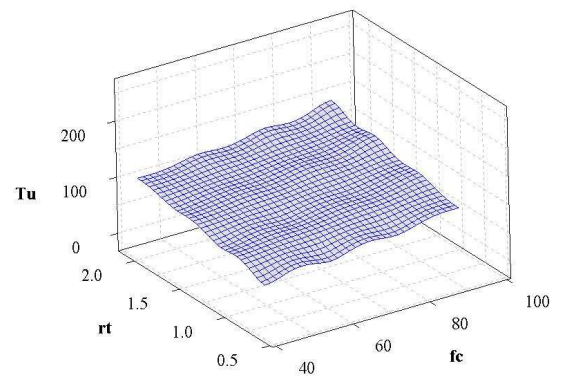
(b)

Surface Plot of Tu vs rt, Pc



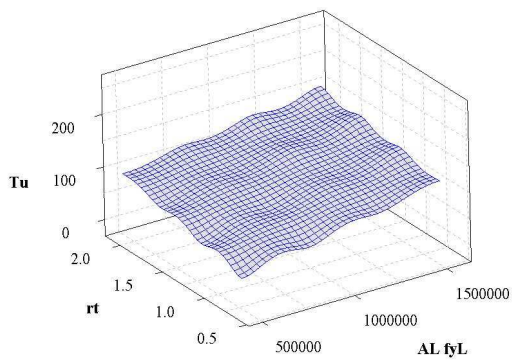
(c)

Surface Plot of Tu vs rt, fc



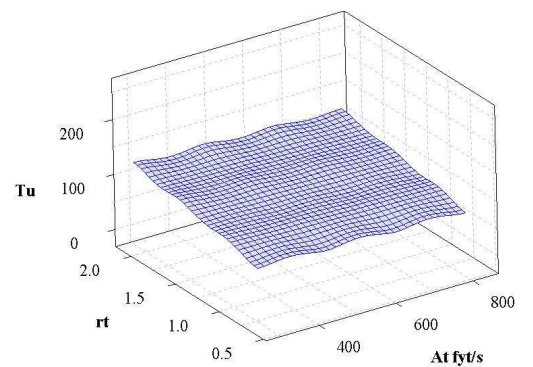
(d)

Surface Plot of Tu vs rt, AL fyL



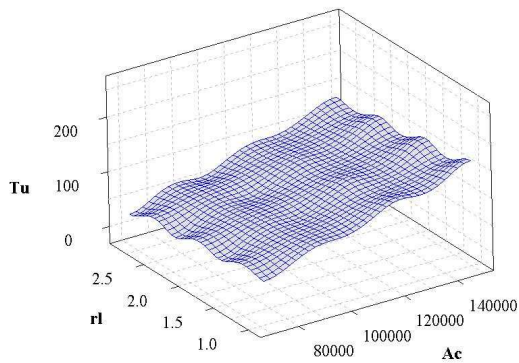
(e)

Surface Plot of Tu vs rt, At fy/s



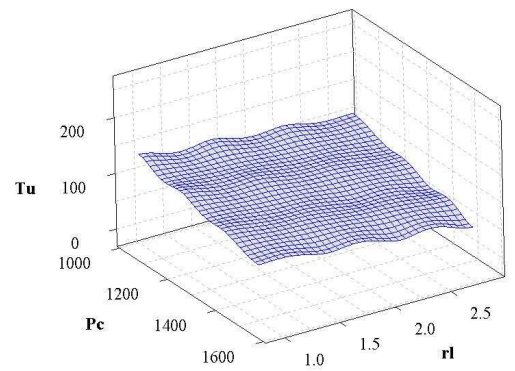
(f)

Surface Plot of Tu vs rl, Ac



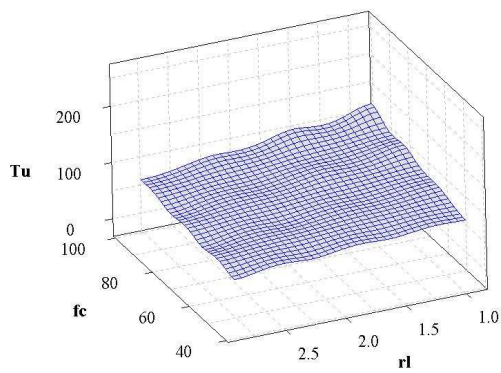
(g)

Surface Plot of Tu vs rl, Pc



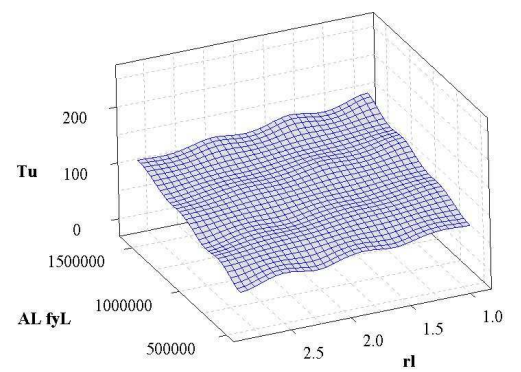
(h)

Surface Plot of Tu vs rl, fc



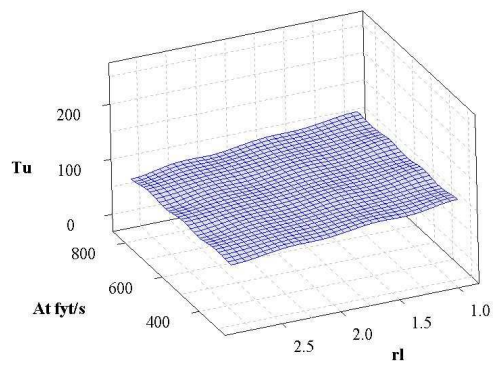
(i)

Surface Plot of Tu vs rl, AL fyL

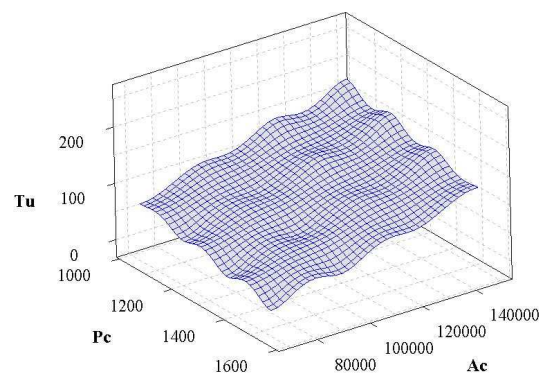


(j)

Surface Plot of Tu vs rl, At fyt/s

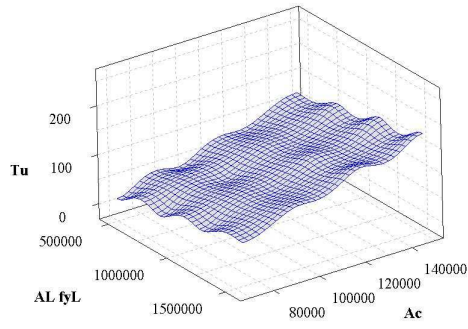


Surface Plot of Tu vs Ac, Pc



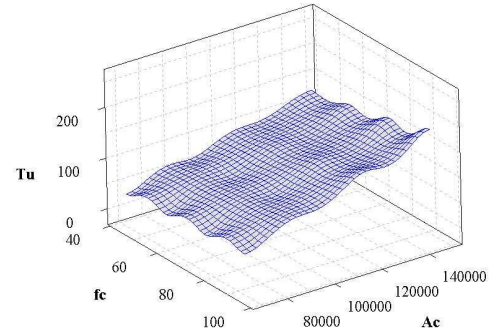
(k)

Surface Plot of Tu vs Ac, AL fyL



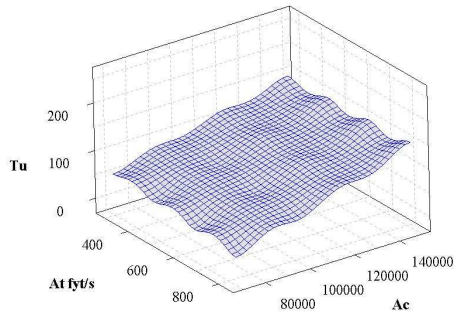
(l)

Surface Plot of Tu vs Ac, fc



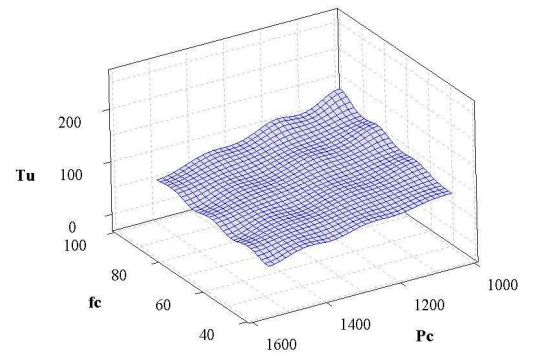
(m)

Surface Plot of Tu vs Ac, At fyL/s



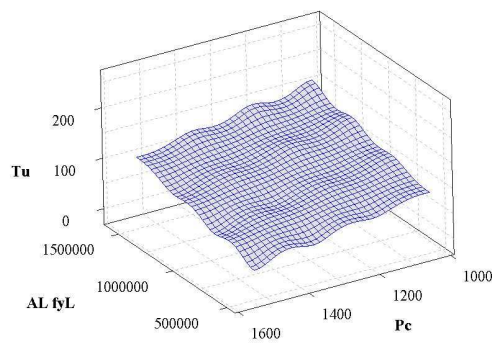
(n)

Surface Plot of Tu vs Pc, fc



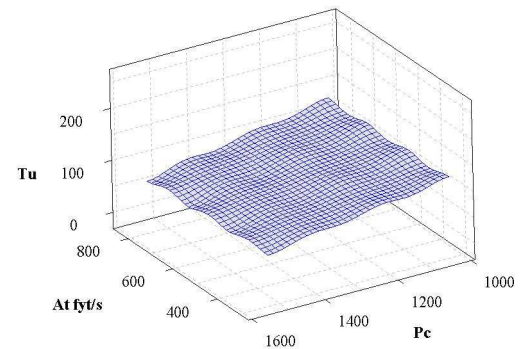
(o)

Surface Plot of Tu vs Pc, AL fyL



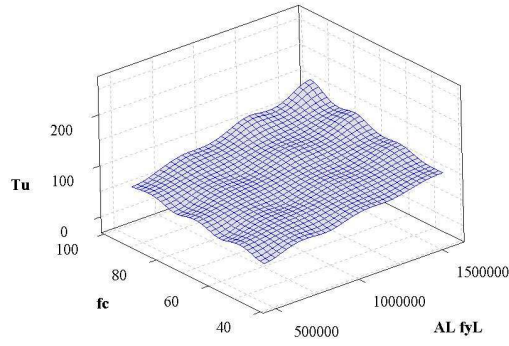
(p)

Surface Plot of Tu vs Pc, At fyL/s



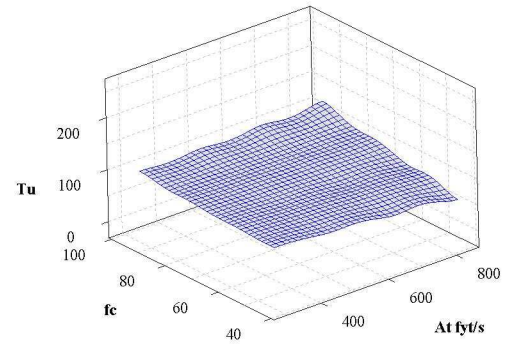
(r)

Surface Plot of Tu vs fc, AL fyL



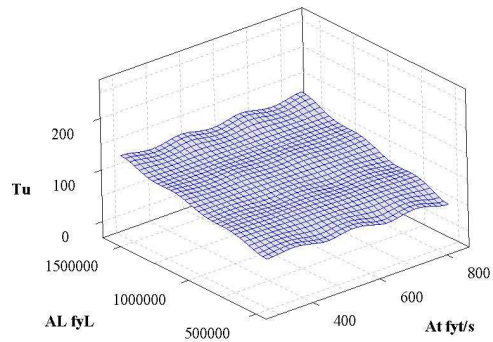
(t)

Surface Plot of Tu vs fc, At fyt/s



(u)

Surface Plot of Tu vs AL fyL, At fyt/s



(v)

Fig5.8 3D Parametric Study for NN model 2

CHAPTER 6

CONCLUSION

6.1 Conclusion

Analysis of torsional strength can be roughly known as classified into two main categories: the skew-bending and the space-truss analogy theory. The two theories for torsional strength of reinforced concrete members are reviewed briefly. On the other hand, the ACI Building Code provisions for torsional design were selected and used in this study for comparison with the results from the NN models. Torsion rarely occurs in concrete structures without being accompanied by bending and shear. The foregoing should give a sufficient background on the contribution of the plain concrete in the section toward resisting part of the combined stresses resulting from torsional, axial, shear, or flexural forces.

Artificial Neural Networks (ANN) can be defined as computer models that mimic the biological nervous system in general. There are many definitions of NNs in literature which can be summarized. NN architectures are formed by three or more layers, which includes an input layer, an output layer and a number of hidden layers in which neurons are connected to each other with modifiable weighted interconnections. Each hidden or output neuron receives a number of weighted input signals from each of the units of the preceding layer and generates only one output value. This NN architecture is commonly referred to as a fully interconnected feedforward multi-layer perceptron. The number of neurons in each layer may vary depending on the problem.

This study presents the application of Neural Networks (NN) for modeling torsion of RC beams. The proposed soft computing models are actually empirical based on a wide range of experimental database collected from the literature. For comparative analysis, numerical results of the same database are obtained by an existing model available in the literature. The proposed NN models are found to be more accurate.

To verify the generalization capability of the proposed NN model a wide range of parametric studies are performed in 2D and 3D form. Verification with the experimental results showed that the proposed NN models can be effectively used for the torsional strength prediction of RC beams.

6.2 Recommendations for Further Work

The problem considered in the thesis can be studied using other soft computing techniques such as Neuro-fuzzy, Genetic programming and Stepwise Regression.

APPENDIX A

1. NN Model 1 Data

No	Ac	Pc	fc	Alfyl	AtFyt/s	Tu	Tu(NN)
1	175000	1700	78,5	526504	313,852	92	106,128
2	175000	1700	78,5	831152	313,852	115,1	123,664
3	175000	1700	78,5	831152	627,704	155,3	151,688
4	175000	1700	78,5	1,49E+06	627,704	196	184,704
5	175000	1700	78,5	1,93E+06	1013,6	239	218,427
6	175000	1700	68,4	859500	332,873	126,7	116,049
7	175000	1700	68,4	859500	570,15	135,2	136,908
8	175000	1700	68,4	1,43E+06	348,724	144,5	149,41
9	175000	1700	35,5	524304	313,852	79,7	72,8473
10	175000	1700	35,5	831152	313,852	95,2	85,7032
11	175000	1700	35,5	831152	627,704	116,8	109,763
12	175000	1700	35,5	1,49E+06	627,704	138	139,819
13	175000	1700	35,5	1,93E+06	1013,6	158	179,069
14	175000	1700	35,5	859500	332,873	111,7	88,3921
15	175000	1700	35,5	859500	570,15	125	106,656
16	175000	1700	35,5	1,43E+06	332,873	117,3	115,167
17	61915	1016	39,6	195625	246,353	19,4	16,4548
18	61915	1016	64,6	195625	263,525	18,9	16,6253
19	61915	1016	75	195625	246,353	21,1	16,2652
20	61915	1016	80,6	195625	263,525	19,4	16,8037
21	61915	1016	93,9	195625	254,939	21	17,031
22	61915	1016	76,2	195625	269,935	18,4	16,8859
23	61915	1016	72,9	242249	289,825	22,5	17,7812
24	61915	1016	75,9	283555	305,926	23,7	18,6995
25	61915	1016	76,7	301872	393,334	24	21,639
26	44000	870	41,7	957218	580,323	16,6	21,9054
27	44000	870	38,2	985008	583,814	15,3	22,4858
28	44000	870	36,3	934060	586,432	15,3	22,052
29	44000	870	61,8	944867	580,323	20	21,4247
30	44000	870	57,1	947955	580,323	18,5	21,4715
31	44000	870	61,7	944867	580,323	19,1	21,4244
32	44000	870	77,3	952586	574,215	20,1	21,6811
33	44000	870	76,9	947955	572,469	20,7	21,5264
34	44000	870	76,2	952586	578,578	21	21,8038
35	44000	870	109,8	943562	571,597	24,7	25,4105
36	44000	870	105	967991	575,96	23,6	25,1233
37	44000	870	105,1	971113	571,597	24,8	24,995

38	96774	1270	27,58	159365	159,739	22,3	26,3058
39	96774	1270	28,61	200958	223,82	29,3	28,7115
40	96774	1270	28,06	249555	319,164	37,5	32,3958
41	96774	1270	30,54	284409	444,632	47,3	38,0639
42	96774	1270	29,03	337647	582,385	56,2	45,0876
43	96774	1270	28,82	379065	714,725	61,7	52,9097
44	96774	1270	25,99	162519	317,788	26,9	30,7265
45	96774	1270	26,75	163571	708,634	32,5	46,5652
46	96774	1270	28,82	243253	284,884	29,8	31,2459
47	96774	1270	26,48	382219	284,31	34,4	33,2118
48	96774	1270	26,61	169174	158,124	22,4	26,3001
49	96774	1270	25,58	204895	231,537	27,7	28,6852
50	96774	1270	28,41	260353	332,233	40,2	33,0693
51	96774	1270	30,61	293601	457,632	47,9	38,7972
52	96774	1270	29,85	207086	168,542	30,4	27,3514
53	96774	1270	30,54	250607	242,855	40,6	30,2151
54	96774	1270	26,75	286249	295,772	43,8	32,046
55	96774	1270	26,54	323637	394,727	49,6	36,2417
56	96774	1270	27,99	383008	507,644	55,7	42,4474
57	96774	1270	29,37	727241	617,368	60,1	57,3776
58	96774	1270	45,23	206648	252,382	36	31,6788
59	96774	1270	44,75	261640	332,922	45,6	35,4747
60	96774	1270	44,95	280115	448,15	58,1	40,6636
61	96774	1270	45,02	315224	589,871	70,7	48,3724
62	96774	1270	45,78	371966	728,481	76,7	57,9623
63	129032	1524	29,79	163571	129,048	26,8	34,5129
64	129032	1524	30,89	204895	197,212	40,3	37,9426
65	129032	1524	26,82	257960	266,501	49,6	40,9118
66	129032	1524	28,27	289307	379,08	64,9	47,027
67	129032	1524	26,89	336245	483,053	72	53,1872
68	129032	1524	29,92	382554	348,734	39,1	48,4511
69	129032	1524	30,96	456499	279,824	52,7	47,3299
70	129032	1524	28,34	552535	397,227	63,3	55,3459
71	129032	1524	27,03	130031	112,757	11,3	32,9148
72	129032	1524	26,54	169875	209,101	15,3	36,8022
73	129032	1524	26,89	210153	298,901	20	41,2071
74	129032	1524	27,17	256383	420,834	25,3	47,8892
75	129032	1524	27,23	291761	569,25	29,7	56,7056
76	129032	1524	27,58	320832	766,992	34,2	69,762

APPENDIX B

1. NN Model 2 Data

No	rt	rl	Ac	Pc	f'c	Al fyl	At fyt/s	Tu	Tu(NN)
1	0,61	0,68	175000	1700	78,5	526504	313,852	92	96,2325
2	0,61	1,16	175000	1700	78,5	831152	313,852	115,1	111,722
3	1,22	1,16	175000	1700	78,5	831152	627,704	155,3	151,254
4	1,22	1,64	175000	1700	78,5	1,49E+06	627,704	196	193,74
5	1,97	1,96	175000	1700	78,5	1,93E+06	1013,6	239	236,072
6	0,68	0,98	175000	1700	68,4	859500	332,873	126,7	115,964
7	1,36	0,98	175000	1700	68,4	859500	570,15	135,2	147,601
8	0,68	1,64	175000	1700	68,4	1,43E+06	348,724	144,5	146,69
9	0,61	0,68	175000	1700	35,5	524304	313,852	79,7	82,4712
10	0,61	1,16	175000	1700	35,5	831152	313,852	95,2	93,1348
11	1,22	1,16	175000	1700	35,5	831152	627,704	116,8	108,292
12	1,22	1,64	175000	1700	35,5	1,49E+06	627,704	138	136,837
13	1,97	1,96	175000	1700	35,5	1,93E+06	1013,6	158	159,498
14	0,68	0,98	175000	1700	35,5	859500	332,873	111,7	101,94
15	1,36	0,98	175000	1700	35,5	859500	570,15	125	120,243
16	0,68	1,64	175000	1700	35,5	1,43E+06	332,873	117,3	123,004
17	0,92	0,82	61915	1016	39,6	195625	246,353	19,4	18,1043
18	0,92	0,82	61915	1016	64,6	195625	263,525	18,9	18,443
19	0,92	0,82	61915	1016	75	195625	246,353	21,1	18,9141
20	0,92	0,82	61915	1016	80,6	195625	263,525	19,4	17,7642
21	0,92	0,82	61915	1016	93,9	195625	254,939	21	17,978
22	0,98	0,82	61915	1016	76,2	195625	269,935	18,4	20,5048
23	1,05	1,05	61915	1016	72,9	242249	289,825	22,5	21,469
24	1,11	1,23	61915	1016	75,9	283555	305,926	23,7	22,4442
25	1,42	1,28	61915	1016	76,7	301872	393,334	24	34,3973
26	1,49	3,51	44000	870	41,7	957218	580,323	16,6	16,1633
27	1,49	3,51	44000	870	38,2	985008	583,814	15,3	16,1722
28	1,49	3,51	44000	870	36,3	934060	586,432	15,3	12,9608
29	1,49	3,51	44000	870	61,8	944867	580,323	20	18,4958
30	1,49	3,51	44000	870	57,1	947955	580,323	18,5	18,3223
31	1,49	3,51	44000	870	61,7	944867	580,323	19,1	18,4903
32	1,49	3,51	44000	870	77,3	952586	574,215	20,1	19,6692
33	1,49	3,51	44000	870	76,9	947955	572,469	20,7	19,4946
34	1,49	3,51	44000	870	76,2	952586	578,578	21	19,4217
35	1,49	3,51	44000	870	109,8	943562	571,597	24,7	23,458
36	1,49	3,51	44000	870	105	967991	575,96	23,6	23,5211
37	1,49	3,51	44000	870	105,1	971113	571,597	24,8	23,876

38	0,54	0,52	96774	1270	27,58	159365	159,739	22,3	20,9669
39	0,81	0,66	96774	1270	28,61	200958	223,82	29,3	29,8102
40	1,15	0,79	96774	1270	28,06	249555	319,164	37,5	39,7968
41	1,59	0,92	96774	1270	30,54	284409	444,632	47,3	50,382
42	2,09	1,05	96774	1270	29,03	337647	582,385	56,2	55,2601
43	2,56	1,18	96774	1270	28,82	379065	714,725	61,7	52,8632
44	1,15	0,52	96774	1270	25,99	162519	317,788	26,9	37,3512
45	2,56	0,52	96774	1270	26,75	163571	708,634	32,5	38,6756
46	0,96	0,79	96774	1270	28,82	243253	284,884	29,8	32,7455
47	0,96	1,18	96774	1270	26,48	382219	284,31	34,4	34,8361
48	0,54	0,52	96774	1270	26,61	169174	158,124	22,4	21,5674
49	0,81	0,66	96774	1270	25,58	204895	231,537	27,7	28,8474
50	1,15	0,79	96774	1270	28,41	260353	332,233	40,2	39,1589
51	1,59	0,92	96774	1270	30,61	293601	457,632	47,9	49,3728
52	0,55	0,66	96774	1270	29,85	207086	168,542	30,4	21,2939
53	0,79	0,79	96774	1270	30,54	250607	242,855	40,6	28,1115
54	1,05	0,92	96774	1270	26,75	286249	295,772	43,8	36,785
55	1,39	1,05	96774	1270	26,54	323637	394,727	49,6	44,6591
56	1,77	1,18	96774	1270	27,99	383008	507,644	55,7	52,6466
57	2,09	2,36	96774	1270	29,37	727241	617,368	60,1	64,9097
58	0,84	0,66	96774	1270	45,23	206648	252,382	36	29,9316
59	1,15	0,79	96774	1270	44,75	261640	332,922	45,6	42,5723
60	1,59	0,92	96774	1270	44,95	280115	448,15	58,1	56,7423
61	2,09	1,05	96774	1270	45,02	315224	589,871	70,7	68,4014
62	2,56	1,18	96774	1270	45,78	371966	728,481	76,7	74,1265
63	0,4	0,39	129032	1524	29,79	163571	129,048	26,8	25,8526
64	0,63	0,49	129032	1524	30,89	204895	197,212	40,3	34,4545
65	0,87	0,59	129032	1524	26,82	257960	266,501	49,6	45,0331
66	1,18	0,69	129032	1524	28,27	289307	379,08	64,9	53,6164
67	1,57	0,79	129032	1524	26,89	336245	483,053	72	65,8144
68	1,06	0,89	129032	1524	29,92	382554	348,734	39,1	51,939
69	0,92	1,11	129032	1524	30,96	456499	279,824	52,7	49,7232
70	1,28	1,33	129032	1524	28,34	552535	397,227	63,3	63,9434
71	0,22	0,3	129032	1524	27,03	130031	112,757	11,3	17,8361
72	0,41	0,39	129032	1524	26,54	169875	209,101	15,3	21,5712
73	0,61	0,49	129032	1524	26,89	210153	298,901	20	25,9331
74	0,86	0,59	129032	1524	27,17	256383	420,834	25,3	30,3319
75	1,16	0,69	129032	1524	27,23	291761	569,25	29,7	32,7694
76	1,57	0,79	129032	1524	27,58	320832	766,992	34,2	31,5672

REFERENCES

ACI Committee 318-71.(1971).*Building code requirements for structural concrete and commentary*. American Concrete Institute, Detroit.

ACI Committee 318-89 .(1989).*Building code requirements for structural concrete and commentary*. American Concrete Institute, Detroit.

ACI Committee 318-95.(1995).*Building code requirements for structural concrete and commentary*. American Concrete Institute, Detroit.

ACI Committee 318-99 .(1999). "*Building code requirements for reinforced concreated*".

ACI Committee 318-2005.(2005).*Building Code Requirements for Structural Concrete(ACI318-05) and Commentary (318R-05)*. American Concrete Institute, Farmington Hills,Mich.

Arslan M.H, Ceylan M, Kaltakçı MY, Ozbay Y, Gulay G. (2007), "Prediction of Force Reduction Factor R of prefabricated Industrial Buildings Using Neural Networks", *Structural Engineering and Mechanics*, **27**, 117-134.

Arslan M.H (2010), Prediction of torsional strength RC beams by using different artificial neural network algorithms and building codes Original Research Article *Advances in Engineering Software* ,**41**, 946-955.

Arthur H. Nilson and George Winter (1991). *Design of Concrete Structures*.McGraw-Hill, Inc.

AS3600 (2001) Concrete Structures, Standarts Association of Australia.

Ayyub, B.M. (1997). *Uncertainty Modeling and Analysis in Civil Engineering*, CRC Press.

BS8110 (1985). Structural Use of Concrete-Part 2. British Standards.

Canadian Standard Association (1994). Design of Concrete Structures: Structure Design. CSA Standard, A23-3-94, Canadian Standard Association, Rexdale, Ontario.

Chao-Wei Tang (2006). Using Radial Basis Function Neural Networks to Model Torsion Strength of Reinforced Concrete Beams. *Computers and Concrete* ,**3**, 335-355.

Chen HM., Tsai KH., Qi GZ. Yang JCS (1995). Amini F. “Neural networks for structural control”, *Journal of Computational Civil Engineering* 9 , **2** , 168–176.

Collins CD, Walsh PF, Archer FE, Hall AS (1965). *Reinforced concrete beams subjected to combined torsion and shear*. UNICIV Report, No.R-14, University of New South Wales.

Çevik A. (2006). *A New Approach for Elastoplastic Analysis of Structures ; Neural Networks*. Ph.D Thesis, Turkey: University of G.Antep.

Çevik A, Küçük M.A, Erklig A, Güzelbey İ.H.(2008).Neural Network Modelling of Arc Spot Welding.*Journal of Materials Processing Technology* ,**202**, 137-144.

Çevik A, Güzelbey İ.H. (2008).Neural Network Modelling of Strength Enhancement for CFRP Confined Concrete Cylinders.*Building and Environment* ,**43**, 751-763.

Çabalar A.F.,Çevik A. (2009).Modelling Damping Ratio and Shear Modulus of Sand-Mica Mixtures Using Neural Networks.*Engineering Geology* ,**104** , 31-40.

Çevik A, Arslan M.H, Köroğlu M.A. (2010). Genetic Programming Based Modeling of Torsional Strength of RC Beams.*KSCE Journal of Civil Engineering* ,**14**,371-384.

Edward G.Nawy.(2005).*Reinforced Concrete A Fundamental Approach*.(5th ed).
Prentice Hall International Series. William J. Hall Editor.

Elcordy MF. Chang KC. and Lee GC. (1993)“Neural networks trained by
analytically simulated damage states”, *Journal of Computational Civil Engineering* 7
,**2**, 130–145.

Elfegren L, Karlsson I, Losberg A. (1974).Torsion bending-shear interaction for
concrete beams. *Journal of Structural Division ASCE*,**100**, 1657-1676

European Standard. Eurocode 2(2002): *Design of Concrete Structures*,Draft for stage
49,Commission of the European Communities, European Committee for
Standardization.

Fang IK. and Shiau JK., (2004).“Torsional Behavior of Normal and High Strength
Concrete Beams” *ACI Structural Journal*,**101**, 304-313.

Gallagher, R. S. (1995). *Computer Visualization: Graphics Techniques for Scientific
and Engineering Analysis*, CRC Press.

Güzelbey IH. Cevik A. Erklig A. (2006).Prediction of Web Crippling Strength of
Cold formed Steel Sheeting Using Neural Networks. *Journal of Constructional Steel
Research*,**62**,962-73.

Hajela S. and Berke L.,(1991)“Neurobiological Computational Models in Structural
Analysis and Design” *Computer and Structures, Elsevier Science Ltd.* ,**41**, , 657-667.

Haykin, S. (1994). *Neural Networks: A Comprehensive Foundation*, NY:Macmillan.

Hebb, D.O.(1949). *The Organization of Behavior*. Wiley, New York.

Hecht-Nielsen, R. (1990).*Neurocomputing*, Addison-Wesley, Reading, MA.

Hossain, T. and Mendis, P. and Aravinthan, Thiru and Baker, Graham (2006) "Torsional resistance of high-strength concrete beams" In: 19th *Australasian Conference on the Mechanics of Structures and Materials*.

Hsu TTC. (1968) Torsion of structural concrete-behavior of reinforced concrete Rectangular members. Torsion of Structural Concrete SP-18, ACI, Farmington Hills. Mich.261-306.

Hsu TTC.(1968)Ultimate torque of reinforced concrete members. *Journal of the Structural Division, ASCE*,**94**, 485-510

Hsu, T. T. C. (1983) *Torsion of Reinforced Concrete*, Van Nostrand Reinhold, New York, 510 .

Hsu, T. T. C., (1990) "Shear Flow Zone in Torsion of Reinforced Concrete," *Journal of the Structural Division, ASCE*, **116**, New York, November 3206 - 3225.

Hsu, T. T. C.(1993) *Unified Theory of Reinforced Concrete*. CRC Press. Boca Raton, FL.,313 .

Inel M. (2007), "Modeling ultimate deformation capacity of RC columns using artificial neural Networks", *Engineering Structures, Elsevier Science Ltd.* ,**29**, 329-335.

Jenkins WM., (1997),Approximate analysis of structural grillages using a neural network. *Proc Instn Civil Engrs Structs Buildings* ,**122**,355–363.

Kasabov, K.N. (1996). *Foundations of Neural Networks, Fuzzy Systems, and Knowledge Engineering*,A Bradford Book The MIT Press Cambridge, Massachusetts, London, England

Koutchoukali NE. and Belarbi G., (2001) "Torsion of High Strength Reinforced Concrete Beams and Minimum Reinforcement Requirement" *ACI Structural Journal* ,**98**, 462-469.

Lessig, N. N. (1953). "*Theoretical and experimental investigations of reinforced concrete elements subjected to combined bending and torsion.*" Theory of design and construction of reinforced concrete structures, 73-84.

Lessig NN. (1959). Determination of carrying capacity of reinforced concrete elements with rectangular cross –section subjected to flexure with torsion Zhelezonabetona, **5**,:5-28.

Matlab, (2006), Neural Networks Toolbox User Guide.

McMullen AE. and Rangan BV. (1978), "Pure Torsion in Rectangular Section-A Reexamination" *ACI Journal*, 511-519.

Michael P. Collins, and Denis Mitchell, (1980). "Shear and Torsion Design of Prestressed and Non-Prestressed Concrete Beams," *PCI Journal* ,**25**, 32-100.

Minsky, M. and Pappert, S. (1969). *Perceptrons*. MIT Press, Cambridge, MA.

Moiler AF. (1993) A sealed conjugate gradient algorithm for fast supervised learning. *Neural Networks*,**6**,525-33.

Mukherjee A. Deshpande JM. and Anmada J. (1996) "Prediction of buckling load of columns using artificial neural networks", *Journal of Structural Engineering, ASCE* 122 ,**11**,1385- 1387.

Nadim Hassoun M. (1985), "*Design of Reinforced Concrete Structures*," PWS Engineering, Boston.

Nawy, E. G.(2000). *High Performance Concrete*. (2nd ed). John Wiley & Sons. NewYork. 550 .

Nawy EG. (2003).*Reinforced concrete, a fundamental approach*, Pearson Education.

Nigrin, A. (1993). *Neural Networks for Pattern Recognition*, Cambridge, The MIT Press.

Pala M, Çağlar N, Elmas N, Çevik A, Sarıbıyık M. (2008). Dynamic Soil Structure Interaction Analysis of Buildings by Neural Networks. *Construction and Building Material*, **22**, 330-342.

Phatak. D. R, and Dhonde. H. B. (1999). "Discussion of 'Behavior of five large spread footings in sand", by Jean-Louis Briaud and Robert Gibbens." *J. Geotech. Geoenviron. Eng.*, **126**, 940-942.

Rafiq MY. (2001). Bugmann G., and Easterbrook DJ., Neural network design for engineering applications *Computers & Structures, Elsevier Science Ltd.*, **79**, 1541-1552.

Rasmussen LJ. and Baker G. (1995). "Torsion in Reinforced Normal and High Strength Concrete Beams Part-I : An Experimental Test Series" *ACI Structural Journal*, **92**, 56-62.

Rausch, E. (1929). *Design of reinforced concrete for torsion and bending*. Springer Verlag. Berlin.

Rumelhart, D.E., Hinton, G.E. and Williams, R.J. (1986). *Learning internal representation by error propagation*. *Parallel Distributed Processing: Exploration in the Microstructure of Cognition*, **1**, Chapter 8, MIT Press, Cambridge, MA

Tapkın S, Çevik A, Uşar Ü. (2010). Prediction of Marshall Test Results for Polypropylene Modified Dense Bituminous Mixtures Using Neural Networks. *Expert Systems with Applications*, **37**, 4660-4670.

TBC-500 (2000): *Requirements for Design and Construction of Reinforced Concrete Structures*, Turkish Standards TS-500.

Thurliman, B.(1979) *Torsional Strength of Reinforced and Prestressed Concrete Beams CEB Approach*, U.S. and European Practices, Special Publication. American Concrete Institute Farmington Hills, MI, 117-143.

Topping, B.H.V. and Bahreininejad, A. (1997). *Neural Computing For Structural Mechanics*, Saxe-Coburg Publications

Wang, W.. and Hsu, T. T. C. (1997). "Limit analysis of reinforced concrete beams subjected to pure torsion." *J. Struct. Eng.*, **123**, 86-94.

Wasserman, P.D. (1989). *Neural Computing Theory and Practice*. Van Nostrand Reinhold Co. New York.

Waszczyszyn, Z. (1999). *Neural networks in the analysis and design of structures*. CISM Courses and Lectures no. 404. New York: Springer.

Waszczyszyn, Z. and Ziemiański, L. (2001). Neural networks in mechanics of structures and materials—new results and prospects of applications, *Comput Struct* **79**, 2261–2276.

Waszczyszyn, Z. (2000a). "Neural networks in plasticity: some new results and prospects of applications", *European Congress on Computational Methods in Applied Sciences and Engineering, ECCOMAS*.

www.comp.nus.edu.sg

Victor DJ. and Muthukrishnan R.(1973). "Effect of Stirrups on Ultimate Torque of Reinforced Concrete Beams" *ACI Journal*, 70-32 , 300-306.

Yudin, V. K. (1962). "Determination of the load-carrying capacity of rectangular reinforced concrete elements subjected to combined torsion and bending.(Concrete and Reinforced Concrete), **6** , 265-269.

Yunjing Zhang. (2002) Torsion in High Strength Concrete Rectangular Beams.

Zang Y. (2002)“*Torsion in High Strength Concrete Rectangular Beams*” Master thesis, University of Nevada.

Zeng, P.(1998). Neural Computing in mechanics, *Appl. Mech. Rev.*,**51** ,173-197

Zia P, Hsu, TTC. (2004) Design for torsion and shear in prestressed concrete. Precast/Prestressed Concrete Institute, *PCI Journal* ,**49**, 34-42.

Zurada, J.M. (1992), *Introduction to Artificial Neural Systems*, Boston:PWS Publishing Company.

Zupan, J, Gasteiger J. (1993). *Neural Networks for Chemists - An Introduction*; VCH: Weinheim.

